Research Article **ISSN: 2349 – 7106**

Asian Journal of Research in Chemistry and Pharmaceutical Sciences

Journal home page: www.ajrcps.com

https://doi.org/10.36673/AJRCPS.2022.v10.i02.A10

THEORETICAL AND DFT STUDIES OF 4-((*E*)-(4-AMINOPHENYL)DIAZENYL)-2-((*E*)-(PYRIDIN-2-YLIMINO)METHYL)PHENOL AND N-(4-((*E*)-(4-HYDROXY-3-((*E*)-(PYRIDIN-2-YLIMINO)METHYL)PHENYL)DIAZENYL)PHENYL)ACETAMIDE

S. Richard Rajkumar[1], G. Vallal Perumal[2], G. Rajarajan[2], V. Periyanayagasamy[1], V. Thanikachalam*[2]

[1]Department of Chemistry, St. Joseph's College of Arts and Science (Autonomous), Cuddalore-1, Tamilnadu, India.

[2*]Department of Chemistry, Annamalai University, Annamalainagar-608002, Tamilnadu, India.

ABSTRACT

Theoretical calculation of 4-((*E*)-(4-amino-phenyl)diazenyl)-2-((*E*)-(pyridin-2-ylimino) methyl) phenol (1) and N-(4-((*E*)-(4-hydroxy-3-((*E*)-(pyridin-2-ylimino)methyl)phenyl)diazenyl)phenyl)acetamide (2) were studied by DFT/B3LYP//6-311+G(d,p) basis set. The calculated values of geometric structural parameters, FT-IR spectral data, HOMO-LUMO, NBO, NISC, Fukui function, polarisability, hyperpolarisability and UV data of compounds 1 and 2 clearly indicate that substitution on amino group alters the physical properties of the compound 2. The NICS value of amino-substituted phenyl ring reduce the aromatic character due to lone pair electron on nitrogen involved in inductive, conjunction effect and also due to OH, NH_2 and OH, $NHCOCH_3$ in compounds 1 and 2, respectively. Solvent effect on different parameters were studied and found that increasing dielectric constant increases the studied parameter. The stability and planarity of the molecule's effects on dipole moment, energy, polarisablity and hyperpolarisablity were studied vastly.

KEYWORDS

HOMO-LUMO, NBO, Polarisability, Hyperpolarisability, Solvent effect, UV-Vis studies, Dihedral angles, Energy, Stability, Dipole moment, Fukui function, HOMA and NICS.

Author for Correspondence:

Thanikachalam V,
Department of Chemistry,
Annamalai University, Annamalainagar,
Tamilnadu, India.

Email: pvta1998@yahoo.co.in

INTRODUCTON

Method for the formation of imines are attractive to synthetic chemists due to exists of this structural unit in a variety of naturally and pharmacologically great molecules[1-3] and similarly for other references. Different broad-spectrum biological activities like anti-proliferative[4,5] anti-inflammatory[6,7], analgesic[8], antimicrobial[9], antiviral[10], anticonvulsant[11], antifungal[12], antimalarial[13], antitubercular[14], antibacterial[15], antioxidant[16], anthelmintic[17] etc.

Prevail in the properties of azomethines. It is act as good Mannich electrophiles and excellent hetero dienophiles for the construction of six-membered nitrogen heterocycles[18,19] Azomethines with pyridine structure appear in agrochemicals and pharmaceuticals[20-23]. From the above facts, no report on theoretical study of 4-((*E*)-(4-amino-phenyl)diazenyl)-2-((*E*)-(pyridin-2-ylimino)methyl)phenol (1) and theoretical and experimental N-(4-((*E*)-(4-hydroxy-3-((*E)*-(pyridin-2-ylimino)methyl)phenyl)diazenyl)-phenyl)acetamide (2) were studied by DFT/B3LYP//6-311+G (d,p) basis set.

MATERIAL AND METHODS

4-N-Acetylaminoanilide, salicylaldehyde, 2-aminopyridine, sodium hydroxide, sodium carbonate, sodium nitrite, and concentrated HCl were purchased from sd-fine chemicals, India. AnalaR solvents were used as such without further purifications.

General Procedure

One equivalent of 4-N-acetylaminoanilide and 1.2 equivalent sodium nitrite and conc. HCl cooled to 0^{o}C and added one equivalent of salicylaldehyde in 10% NaOH with constant stirring for about 1 hour. The resultant product was neutralized conc. HCl using methyl red paper. The reddish-brown product was isolated and recrystallized with ethanol. To the product obtained 2-aminopyridine was condensed to yield the final product, N-(4-((*E*) (4-hydroxy-3-((*E*) (pyridine-2-ylimino)methyl)-phenyl)diazenyl)phenyl)acetamide 2. It was characterized by microanalysis. %C: 66.80(66.84); %N: 19.42(19.49); %H.4.72(4.77) and FT-IR spectrum and data are displayed in Tables No.1 and Table No.2 (Figure No.2).

Detection Method

FTIR spectrum of N-(4-((*E*)(4-hydroxy-3-((*E*)-(pyridine-2-ylimino) methyl)-phenyl) diazenyl) phenyl) acetamide (2) was recorded on a Bruker IFS 66V spectrometer equipped with a Globar source, Ge/KBr beam splitter and a TGS detector in the range of 4000-400 cm^{-1}. The spectral resolution is ±2 cm^{-1}.

The theoretical study of compounds 1 and 2 was carried out using the Gaussian 09W and the output files are visualized by Gauss View 5.0 software. The structural parameters, FTIR frequencies, and HOMO-LUMO energies are calculated using DFT methods with B3LYP/ 6-311+G(d,p) basis set. The vibration frequencies are obtained by the DFT method and are scaled-down by using scaling factors 0.961 and 0.958.[24] the vibrational assignments of compounds 1 and 2 are using the Veda-4[25] program. The NBO analysis was performed by utilizing NBO 3.1 program in the Gaussian 09W at B3LYP/6-311+G(d,p) method. To investigate the reactive sites (charged region of a molecule), molecular electrostatic potential (MEP) were evaluated using the above method.

RESULTS AND DISCUSSION

Optimized Parameters

DFT was used to optimise compounds 1 and 2 using the B3LYP/6-311+G(d, p) basis set. The calculated structural parameters are given in Table Nos.S1 and S2 in accordance with the atomic numbering scheme given in Figures No.1.

Both compounds consist of two rings, aniline or anilide ring (1) and phenoxy ring (2) connected to one another by azo chromophore group (-N=N-). The azo aniline ring (1) [N12-N11-C3-C2 = 0.4° and N12-N11-C3-C4 = -179.7°] moiety and phenoxy ring (2) [N11-N12-C13-C14 = 0.3° and N11-N12-C13-C15 = -179°] in 1 are coplanar with the azo chromophore, evident from dihedral angle observation. Similar observation is made in 2 also with little disturbance in dihedral angle of anilide ring (1), the azo anilide ring (1) [N20-N19-C3-C2 = 141.3° and N20-N19-C3-C4 = 145.9°] moiety and phenoxy ring (2) [N19-N20-C21-C22 = -179.4° and N19-N20-C21-C23 = 179.5°] in 2 are coplanar with the azo chromophore. The OH group in both compounds are para to the azo nitrogen's and they are in plane in C2 with nitrogen from 2-aminopyridine moiety. [H31-O30-C28-C24 = 0.8° and N34-C32-C24-C28 = 0.7°] in 2. C16-C20-O22-H23 = -7.9° and C20-C16-C27-N29 = 173.9°] in compound 1, where the planarity is found to be disturbed. It explicit to note that the O30-H31 group

in 2 is coplanar with N34. This paves way for stronger hydrogen bonding in 2 and hydrogen bonding is expected to be missing in 1 because of loss of planarity and it is realised from bond lengths. The bond lengths of azo N11 and aniline ring (1), azo N12 and phenoxyring (2) in 1 are (ring1) N11-C3 = 1.4059 Å, which is comparatively less than N12-C13, which is 1.4164 Å in ring 2, and this is attributed to intra-molecular charge transfer (ICT) from ring1 to and localization at the azo bond[26]. The bond lengths between the azo N19 and anilide ring(1), azo N20 and phenoxy ring (2) in 2 are (ring1) N19-C3 = 1.4134 Å, which is comparatively larger than 1.4093 Å (N20-C21) in ring 2 and this is attributed to intra-molecular charge transfer (ICT) from ring 2 to and localization at the azo bond. This difference in ICT between the two compounds may be realised in terms of the difference between electron donating amine in 1 and electron withdrawing anilide in 2.[26] when comparing the two ICT in two compounds, it is discovered that ICT is more prevalent in 1. The C-C bonds of the phenyl rings in 1 are in the range of 1.3814-1.4105 Å in ring1 and in ring 2; 1.3836-1.4149 Å, pyridine ring (ring 3) C-C (1.3894-1.4059 Å) and C-N (1.3336-1.3384 Å) respectively in 1 and it is comparable with crystal data from literature[27]. In 2, it ranges from 1.3855-1.4048 Å in the anilide moiety (ring 1) and the phenoxy moiety (ring 2). In 1, it ranges from 1.783-1.4224 Å in the pyridine ring (ring 3) C-C (1.3892-1.404 Å) and C-N (1.3338-1.3369 Å) and is comparable with crystal data from literature.[27] the calculated N=N length in compounds 1 and 2 is 1.2563 Å and 1.3868 Å, and these values are comparable with the literature value of 1.24 Å[27-29]. The decrease in bond length is due to extended π-conjugation in 1, and the increase in bond length in 2 is due to an electron density flow from the phenyl ring into π* of the azo group.

The O-H bond length in 1 and 2 is 0.9621 Å and 0.9963 Å, respectively, which is comparable to the literature value of 0.82 Å.[30] C32=O33 in 2 is 1.2185 Å, which is compared with 1.24 Å of literature value.[31] The N29-C27 bond length in compound 1 is 1.275 Å and in its counterpart C32-N34 it is 1.2893 Å and its literature value is 1.273 Å. Here the bond is found to be elongated in 2, which may be due to proton transfer from O30 to N34 originating from hydrogen bonding interaction. The C-O bond length in 1 (C20-O22 = 1.3652 Å) and in 2 (C28-O30 = 1.3325 Å) is compared with 1.356 Å[31]. The decrease in length in 2 throws light on proton transfer from O30 to N34, which results in an increase in double bond character in C28.[27]

FTIR Frequencies Analysis

Vibrational and spectral analysis

The analysis of vibrational spectra is based on the FT-IR spectrum and the vibrational wave numbers computed at the B3LYP/6-311+G(d,p) level. Tables No.1 and 2 (Figure No.2) show the experimental and theoretical spectral values calculated at the B3LYP/6-311+G(d,p) level.

The vibrational analysis is executed on the characteristic vibrations of hydroxyl, azo, amine, imine, and phenyl groups. The free hydroxyl stretching vibration is expected in the region of 3700-3584 cm^{-1}, whereas, the formation of hydrogen bonding can lower the O-H stretching frequency to 3550-3200 cm^{-1} [32,33]. The O-H stretching vibration is observed at 3714 cm^{-1} in 1, whereas in 2, the same stretching is obtained at 3041 cm^{-1}. This lowering of OH stretching is attributed to the existence of hydrogen bonding (O30-H31---N34), which is not found in 1. The calculated value of OH group vibration shows good agreement with the experimental result.

The azo group -C-N=N-C-has two different groups attached at the terminus. Depending on the two groups, the bond length (-C-N=) differs, and its contribution to the dipole is undeniable. The N=N stretching mode is predicted at 1469 cm^{-1} in 1 and at 1494 in 2.[34] C-N stretching vibrations are expected to show up in the region of 1200-1130 cm^{-1} [35,36]. These vibrations shift in wave number and intensity depending on the neighbouring groups, conjugation effects, H-bonding, and molecular tautomerism.[36] C3-N11 and N12-C3 stretching vibrations are predicted at 1242 cm^{-1} and 1106 cm^{-1} in compound 1. The C3-N11 bond is shortened and its wave number is found to be increased. In 2, vibrations for C3-N19 and N20-C21 are at 1242 and 1279 cm^{-1}, respectively. Phenyl ring C-C vibrations are found

in the range of 1594-1120 cm^{-1} for 1 and 2. The imine group C=N vibration in 1 (C29-N29) is at 1639 cm^{-1}, which is comparable with 2 (C32-N34) at 1606 cm^{-1}. The decrease in wave number in 2 is attributed to elongation of the bond due to intra-molecular hydrogen bonding and which is not observed in 1. The N-H vibrations are obtained at 3564-3437 cm^{-1} in 1 and 2. It matches with the experimental value of 3645 cm^{-1} for compound 2.[37]

Mulliken and natural population analysis

Mulliken atomic charge plays a vital role in quantum chemistry because of its influence on electronic structure, molecular polarization, dipole moment, and many molecular properties.[38] Mulliken atomic charges of 1 and 2 calculated at the B3LYP/6-311+G(d, p) level are shown in Table Nos.S3 and S4. Most of the nitrogen atoms and all oxygen atoms exhibit an excess of negative charge in both compounds under investigation. All the hydrogen atoms are positive. From literature, it's noteworthy to denote that the more negative the atomic charges that an atom carries, the more easily the atom can donate its electron to the unoccupied orbital of a metal.[39] Thus, the compounds under investigation have reactive sites for protonation and coordination with metal ions.[40] There is a distribution of positive (hydrogen) and negative (N,O,C) charges in the molecule due to which there is the possibility of a number of intermolecular and intra-molecular hydrogen bonds.[29] In 1, the maximum negative charge is identified as C20, and in 2, C22 produces a maximum of 0.8865 electron density. H28 has the highest positive charge, which is attached to C27. H23 exhibits the lowest positive value and it is connected to O30. N39 and N24 show high electron density, whereas N29, N12 and N11 are positive. In compound 2, H33 shows maximum and H31 shows minimum positive charge.

On comparing the two compounds, there is a sea of electron flow in one and it is found missing in its counterpart because of the electron withdrawing anilide moiety. In 1, the π-conjugation is extended till the phenoxy ring.

NBO analysis

The NBO study was performed using Gaussian 09, DFT B3LYP6-311+ G(d,p). The NBO is an effective study for chemical interpretation of hyperconjugate interaction and electron density movement from filled lone pair electrons. The aim of NBO analysis is to predict donor orbitals, acceptor orbitals, and interaction stabilisation energy, which is a result of second order perturbation theory.[41,42] The most valuable interactions between donor and acceptor are reported in Table Nos.S3 and S4. It is known that larger E^2s represent intensive interaction between donor and acceptor. $E^{(2)}$ also proves the efficacy of conjugation in the molecule. From the Table No.S3 and S4, it is evident that in compound 1, strong interactions are from π to π*, LP to π*, and π* to π*. Maximum energy is noted for π*-C5-C6→π*-C3-C4, π*-C5-C6→π*-C1-C2 and π*-C30-N39→π*-C31-C33 with corresponding energies of 322.73, 247.28 and 255.67 kcal/mol respectively.[43] On comparing 1 with the parent compound, it is evident that the number of interactions are increased in 1 due to increased molecular size and planarity and also the intermolecular hydrogen bonding followed by charge transfer is also absent in the parent compound. On this basis, it is proven that the candidate molecule is an efficient choice for NLO studies. In 2, the interactions with the highest $E^{(2)}$ are LP(1)C24→π*-C32-N34 (61.85) and LP(1)C24→π*-C21-C22 (70.81 kcal/mol).

Molecular electrostatic potential (MEP)

By predicting the charge distribution, the electrophilic and nucleophilic sites in the compound can be assessed using MEP[44]. The interaction of molecules with one another and the solvent is depicted using the charge distribution. The MEP of 1 and 2 are shown in Figure No.3. In compounds 1 and 2, the hydrogen atoms attached to nitrogen and oxygen has less electron density (blue colour) and are sites for nucleophilic attack. The territory around oxygen is electron rich (red colour) and yellow colour) and is suitable for electrophilic attack[45].

Aromaticity

Aromaticity indices are controversial subjects in organic chemistry, though the harmonic oscillator model of aromaticity (HOMA) and the nuclear independent chemical shift (NICS) are the most prominent indices to describe π-electron delocalization in a ring system[46] and they are also used to study intermolecular proton transfer.[47,48]

RING 1: The neutral and anion of 2 have higher negative NICS (Table No.S5) values than the cation, which is a quantitative measure of aromatic character. For neutral moiety, a maximum negative value is observed for 1 Bq and -1 Bq above and below the ring (zz). The decreasing order of NICS is neutral > anion > cation. In ring 2 (the phenoxy ring), however, neutral and anion have higher NICS negative values than cation. A maximum negative value is obtained for 1Bq and -1 Bq in neutral species above and below the ring (zz). The order of NICS is cation < anion < neutral.

Cation and neutral have higher NICS negative values than anion in ring 3 (the pyridine ring). A maximum negative value is obtained for 1 Bq and -1.5 Bq in neutral species above and below the ring (zz). The order of NICS is an anion < neutral < cation.[49]

The NICS value of ring 1 and 2 differs with the order of NICS value of ring 3 and this may be attributed to HOMO and LUMO occupancy in the molecule in different ionic states of the candidate molecule.

HOMA

In compound 1, the order of HOMA (Table No.S6) value is ring 1 > ring 2 > ring 3 in neutral and anionic states. In cationic states, the order changes to ring 2 > ring 3 > ring 1. In compound 2, the order of HOMA is found to be ring 1> ring 2 > ring 3. This order is due to the major contribution to HOMO by rings 1 and 2 in both compounds 1 and 2.[50]

The HOMO contribution is 47% and 23% from ring 1 and 2 in compound 1. In compound 2, HOMO is from 30% and 36% of ring 1 and ring 2 and this is realised in NICS value. LUMO is contributed by azo nitrogen and ring 2 in both compounds, and it displays its efficacy to accept any number of electrons. Ring 3 contributes a negligible amount to HOMO and its HOMA value is reasonably low.[51]

Fukui Function

Parr and Yang[52] provided evidence that majority of frontier-electron density theory of chemical reactivity can be reason out using DFT. Parr and Yang define a Fukui function (fk) to describe electrophilic f^-, nucleophilic f^+ and neutral attack.[53] Fukui values for 1 and 2 are given in Table Nos.S7 and S8. The order of nucleophilic attack is C2>N12>C35>C27>C14>C18>N29>C6>C30>C4> N11>C13>N24>O22>C32>33>15>N39>C20>C1> C5>C3>C16>C31 for compound 1 and for compound 2 it is found to be N44>C5>C6>C28>C23>C21>C38>C40>C35>C2> C37>C36>C3>C22>C4> C26>C24>C1. The order of electrophilic attack is C15>N24>C16>N12>C5>C3>C35>C33>O22>>C6 >N29>C31>C2>C30>C27>C1>C18>C4>C13>C20 >N39>N11>C32>>C14 in 1 and in 2 it is found to follow the order C21>C6>C38>C5>C2>C24>C28>C1>N44>C37> C26>C40>C23>C36>C3>C35>C22>C4. On comparing the nucleophlic site C2 in compound 1 is more prone than N44 in compound 2. C15 on 1 is prone to electrophilic attack than C21 in 2.[54] In compound 1 there is flow of electron as conjugation which increases the Fukui value, whereas the conjugation is not prominent in 2. The most electrophilic site is the one with maximum s^+ and ω^+ while maximum s^- and ω^- shown by most nucleophilic site.[43]

NLO property

The NLO properties of an organic molecule are closely related to the extent of π-conjugation. The increase in conjugation in the molecule increases the non-linear optical properties. Substituting electron-donating and electron-withdrawing groups increases the NLO property. If the donating and withdrawing groups are strong, it would increase the π-conjugation through the entire molecule, which increases the polarisability and hyper-polarisability of the molecule.[55] The compounds under study are non-zero dipole moment components. The compounds under investigation are substituted with different groups which alter the

π-conjugation, resulting in a change in polarisability and hyperpolarisability.[54] The dipole moment, polarisability and hyperpolarisability of the title compound were calculated at the DFT/B3LYP/6-311+G(d,p) level using the Gaussian programme package. Calculated values of the parameters are presented in Table No.4. The results are greater than urea[56] about six times and fourteen times for 1 and 2, respectively. Both compounds have higher dipole, polarisability, and hyperpolarisability values than the literature values.[54] These results show that the title compound can be used as a good non-linear optical material. Compound 2 shows a high value of dipole, polarisability, and hyperpolarisability, and this is attributed to the increased planarity and surface of the molecule.

FMO analysis and Solvent effect on UV-Visible data

The experimental electronic spectrum was recorded for the desired compounds in different solvents. The theoretical electronic spectra of 1 and 2 were calculated in the gas phase and various solvents using the TD-SCF method on B3LYP/6-311+G(d, p) level. The experimental and calculated absorption (A), energy (E), and oscillator strength (f) are shown in Table Nos.S9 and S10.[57,58] In compounds 1 and 2, there are π-conjugations all over the molecule and they are explicitly visible from the electronic spectra. Compound 1 shows two absorption bands at 427.2 nm and 387.9 nm in water corresponding to π -π* and n - π* transitions. The one at 427.2 nm is a HOMO to LUMO transition (90%) with oscillator strength of 0.660 a.u. and energy of 2.90 eV. HOMO-LUMO energy gap (Table No.5; Figure No.4) is found to be smaller in 1 than 2, which proves that 1 can exhibit vast transitions than its counterpart.

Compound 2 also marks two absorption maxima at 400.5 nm and 368.8 nm in water, in which 400.5 nm corresponds to oscillator strength of 1.185a.u and 3.096 eV energy. The solvent interaction increases with an increase in the dielectric constant. This phenomenon gives rise to the absorption maximum in the compound.[59,60]

Compound 1: In HOMO, the distribution pattern shows an asymmetrical contribution with 47% for phenyl ring-1(aniline moiety) and 23% for phenyl ring-2 (phenoxy moiety). The nitrogen (N24) of the amine group contributes 16% to the HOMO. Moreover, the p-p type orbitals from the carbon, nitrogen, and oxygen regions significantly contribute 97% to the HOMO. Thus, the compound shows a more atypical electron distribution of the HOMO set.[61,62]

Similarly, in the LUMO, an asymmetrical contribution is exercised. The phenyl ring-1(aniline moiety) contributes 17% and the phenyl ring-2 (phenoxy moiety) contributes 27%. The azo group eccentrically contributes 35%, with 18% from N11 and 17% from N12. The p-π* type orbitals from the carbon and nitrogen atoms wholly contribute 96.5% to the LUMO. Thus, similar to the HOMO, LUMO also shows an atypical electron distribution.

Compound 2: Unlike 1, the HOMO of 2 exhibits a symmetrical distribution with a 36% contribution from phenyl ring-2(phenoxy moiety) and a 30% contribution from phenyl ring-1(aniline moiety). The O30 oxygen of the hydroxyl group attached to the ring 2 (phenoxy moiety) alone contributes 8% to the HOMO. Moreover, the p-p type orbitals from the carbon, nitrogen and oxygen regions significantly contribute 97.052% to the HOMO.

Similarly, the LUMO also shows a symmetrical distribution with a 22% contribution from ring-1(aniline moiety) and a 27% contribution from ring-2(phenoxy moiety). The azo group alone contributes 38% to the LUMO, with an 18% contribution from N19 and a 20% contribution from N20. The p-p* type orbitals from the carbon and nitrogen atoms wholly contribute 96.7% to the LUMO. Thus, similar to the HOMO, the LUMO also exercises symmetrical distribution. In both compounds, the electron distribution from the phenyl ring-1 is composed mainly of the p-π*-type orbitals. Hence, the absorption corresponds to the π-π* transitions.[63]

The Effect of Solvent on Electronic Transition

The solvent effects on the absorption spectra obtained under different solvents are studied, and their data are reported in Table Nos.S9 and S10. It is obvious that the increase in the dielectric constant increases the dipole moment. Consequently, there is

also a change in the polarisability and the hyperpolarisability. The change in the dielectric constant and dipole moment shows a linear dependency (Table No.S11). The dipole moment is comparatively higher for solvents than for gaseous state. Among solvents, compound 1 in water has the maximum dipole moment (3.6509 Debye) and has the minimum dipole moment (3.0656 Debye) in benzene.

Solvents with larger dielectric constants have greater solvation energy. Consequently, with the increase in the dielectric constant, the dipole moment value is also evaluated. It results in increased interaction between the molecule and the solvent. If the HOMO orbitals attain stabilisation, it will increase the optical gap. LUMO stabilisation by solvent, on the other hand, reduces the optical gap and NLO properties.[39-41]

Compound 2 also follows the same trend under different solvents. Among solvents, compound 2 in water has the maximum dipole moment (5.457 Debye) and has the minimum dipole moment (4.7507 Debye) in benzene. In comparison to 1 and 2, compound 2 exhibits a larger dipole moment, hyperpolarity, polarisability and less solvation energy (Table No.S12). Also, it is evident from the dihedral angle that the planarity of compound 2 is higher than compound 1. The planarity increases the dipole moment. Eventually, it affects its dependent properties.

NMR

^{1}H and ^{13}C spectral values are given in Table No.S13. In 1, aromatic proton signals are found in the range of 6.65 to 8.35 ppm, which is an aromatic region. H17 and H36 are said to be deshielded by the adjacent environment and their signals are shifted to downfield. The H23 signal is obtained at 5.30 ppm, which is due to the shielding of the nucleus by O22. H25 and H26 are at 3.46 and 3.48 due to the electronegativity of nitrogen. H28 at 8.49 ppm and it is said to be deshielded. The signal is down fielded compared to the literature value of 7.326 ppm.[45] ^{13}C NMR shows 16 different signals, representing the presence of different kinds of protons. C1 and C5, C1 signals are shifted to the up field due to the π-conjugation from N39 and N24. In 2, the aromatic protons fall in the aromatic region. H31 shows 13.65 ppm, which is accounted for by the presence of hydrogen bonding with N34. C13 demonstrates the presence of different types of carbon. C1 and C5 carbon signals are seen in the range of 124-125 ppm, which is contrary to comparing the position with compound 1. The carbon adjacent to N34 shows up at 168.4 ppm (C32) due to the deshielding effect[45]. H33 resonances at 8.6ppm, which is deshielded compared to the literature value of 7.326 ppm[45]. The H31 signal is noted at 13.65 ppm and this is due to the existence of hydrogen bonding with N34. Due to hydroxyl group deshielding, the carbon signals in compounds 1 and 2 at 165ppm and 173.91ppm respectively, and the carbon signals attached to amine in 1 (155.59) and amide in 2 (147.17) also towards downfield shift[64]. The carbons directly attached to AZO group give signal C3-151.5 ppm, C13-153.31 ppm in 1, C3-155.14, C21-151.42 ppm in 2, respectively.[59] The second and third carbon in 2-aminopyridine moiety give signal at 173.77, 114.61, in 1, 169.91 and 115.48 ppm in 2, respectively.

Potential energy, dipole moment vs dihedral angle

Potential energy, dipole moment vs dihedral angle are plotted and displayed in Figure No.5. It is obvious that 1 has the lowest energy at dihedral angles 0, 10 and at the lowest energy (angle 0) in 1, the two rings, namely the aniline moiety (ring 1) and phenoxy moiety (ring 2), are parallel to each other and coplanar with the azo group, but the pyridine moiety (ring 3) remains perpendicular to ring 1 and ring 2. The highest energy is noted at angles -89 and 90. At these angles, ring 1 and ring 3 are perpendicular to ring 2 and the azo group is not coplanar with either of the rings, which is a highly strained conformer. In 2, the energy is found to be minimum at dihedral angles of 179.78, 170, and 0. The lowest energy is noted at -179 degrees with the most stable conformer.[68] This conformer is planar with respect to the anilide moiety (ring 1) and phenoxy moiety (ring 2), but the pyridine moiety (ring 3) is not planar with the former rings (1 and 2). The conformer with maximum energy and less

stability is predicted with a dihedral angle of -89.78 and 90.21. The most unstable or conformer with maximum energy possesses all the three rings perpendicular to one another. The rings 1, 2 and 3 are not coplanar with the azo nitrogen group.

Dipole moment

For 1, Figure No.5 displays the dihedral angle vs. dipole moment graph. It shows an increase in dipole moment and energy as the dihedral angle decreases. The maximum and minimum dipole moments are noted at 110 and 0, respectively. The trend of the dipole moment falls in line with the trend left by energy, but with considerable alteration.

For 2, it is clear from Figure No.5b that the energy and dipole moment are inversely proportional to each other. Minimum dipole and maximum dipole moments are noted for dihedral angles of 80.21 and -169.78, respectively.[65]

Thermodynamic properties

Thermodynamic parameters, such as zero-point vibrational energy (ZPVE) and entropy, are presented in Table No.6. The variation in ZPVE seems to be significant. The total energies of 1 and 2 are presented. Of the two compounds, 2 show a minimum total energy of -1196.9 a.u and it is comparatively enjoys stability.[40]

Table No.1: Vibrational wave numbers obtained for compound 1 DFT-B3LYP/6-311+G(d,p) [harmonic frequency (cm^{-1}), IR intensity, Raman activity (Km/mol), reduced masses (amu) and force constants ($mDyneA^{\circ-1}$)]

Mode No	Calculated Frequency	IR Intensity	Raman Activity	Reduced Mass	Force Constant	Vibrational Assignment with >10%PED
1	3714	100.73	413.1	1.07	9.26	ν O22-H23(100)
2	3564	22.70	65.8	1.10	8.81	ν N24-H25(50)+N24-H26(50)
3	3465	89.54	375.9	1.05	7.92	ν N24-H25(50)+N24-H26(50)
4	3111	3.08	95.3	1.09	6.65	ν C14-H17(100)
5	3100	3.34	66.6	1.09	6.61	ν C2-H8(97)
6	3095	7.55	165.8	1.09	6.61	ν C15-H19(27)+N24-H26(50)
7	3091	13.52	44.9	1.10	6.61	ν C31-H34(14)+C33-H37(20)+C35-H38(63)
8	3086	4.62	102.7	1.09	6.56	ν C4-H9(92)
9	3084	11.97	131.5	1.09	6.54	ν C31-H34(70)+C35-H38(25)
10	3080	1.44	711.0	1.09	6.50	ν C15-H19(72)+C18-H21(27)
11	3065	7.43	152.7	1.09	6.44	ν C31-H34(16)+C33-H37(75)
12	3058	22.31	94.6	1.09	6.42	ν C5-H10(92)
13	3051	26.88	74.8	1.09	6.39	ν C1-H7(97)
14	3043	26.67	196.1	1.09	6.36	ν C32-H36(95)
15	2857	74.90	55.5	1.08	5.57	ν C27-H28(100)
16	1639	229.98	10.0	8.34	14.11	ν N29-C27(73)
17	1608	312.94	117.0	1.50	2.44	β H26-N24-H25(63)
18	1594	13.75	192.5	3.09	4.94	ν C1-C2(16)+β H26-N24-H25(19)
19	1586	281.38	1728.8	5.41	8.57	ν C20-C18(20)
20	1566	169.87	50.3	6.04	9.33	ν C15-C13(28)
21	1562	220.57	1053.4	5.45	8.38	ν C31-C33(27)+C32-C35(11)
22	1555	34.94	261.4	6.34	9.66	ν C4-C3(25)+C6-C5(24)
23	1548	43.56	1569.5	5.61	8.48	ν N39-C30(17)+C33-C35(16)+C32-C35(20)+β C31-C33-C35(11)
24	1493	113.97	51.0	3.68	5.17	ν N11-N12(29)+β H7-C1-C2(13)
25	1469	75.25	29.5	3.93	5.35	ν N11-N12(24)

26	1457	100.99	229.7	2.99	4.00	β H21-C18-C20(10)
27	1429	91.17	107.0	2.36	3.10	ν N39-C30(16)+β H34-C31-C33(12)+ H36-C32-N39(27)
28	1407	10.77	110.2	3.42	4.34	ν C1-C2(15)+C5-C4(22)+β H7-C1-C2(11)+H10-C5-C6(13)
29	1393	71.53	480.6	2.08	2.60	β H37-C33-C35(26)+ H38-C35-C33(28)
30	1390	112.80	308.5	4.92	6.10	ν N11-N12(13)+C18-C15(15)+C13-C14(13)+C14-C16(17)
31	1376	20.21	802.6	1.49	1.80	β H28-C27-N29(61)
32	1306	5.94	1017.9	4.94	5.41	ν C1-C2(18)+C2-C3(17)+C6-C5(23)+β H25-N24-C6(13)
33	1298	58.53	3968.0	3.84	4.15	ν C18-C15(12)+C13-C14(15)+C20-C18(15)+C14-C16(14)+β H23-O22-C20(15)
34	1274	0.19	522.9	1.53	1.60	β H7-C1-C2(18)+H8-C2-C1(19)+ H9-C4-C5(20)+ H10-C5-C6(14)
35	1268	2.09	6.6	1.71	1.77	ν N39-C32(31)+β H34-C31-C33(10)+β H36-C32-N39(35)
36	1259	203.03	5344.1	3.05	3.10	ν C5-C4(11)+N24-C6(42)
37	1252	114.14	120.5	1.81	1.82	ν O22-C20(10)+β H23-O22-C20(10)+H19-C15-C18(15)+ H21-C18-C20(12)
38	1242	21.02	1804.5	2.94	2.91	ν N11-C3(10)+C16-C27(10)+N12-C13(11)
39	1232	5.98	83.8	4.99	4.86	ν N39-C32(15)+N39-C30(36)+C33-C35(12)
40	1209	107.91	35.1	4.10	3.85	ν N29-C30(23)+O22-C20(11)
41	1190	47.04	5.2	2.54	2.31	ν C14-C16(10)+N11-C3(13)+O22-C20(17)+β H17-C14-C16(21)
42	1175	184.95	1.7	2.69	2.38	β H23-O22-C20(15)+ C13-C14-C16(11)
43	1125	386.57	41.5	1.28	1.04	β H23-O22-C20(20)+H8-C2-C1(11)
44	1122	7.76	9.3	1.15	0.93	ν C33-C35(12)+β H34-C31-C33(21)+H37-C33-C35(36)+H38-C35-C33(19)
45	1121	72.22	10.7	1.35	1.09	β H19-C15-C18(13)+H21-C18-C20(27)
46	1106	19.32	195.4	2.06	1.62	ν N12-C13(16)+β H9-C4-C5(15)
47	1095	5.72	17.1	1.25	0.96	β H25-N24-C6(12)+H7-C1-C2(17)+H8-C2-C1(17)+H10-C5-C6(13)
48	1070	1.58	4.5	1.52	1.12	ν C31-C33(15)+C32-C35(13)+β H34-C31-C33(13)+ H38-C35-C33(32)
49	1055	10.07	0.3	1.88	1.35	ν C20-C18(10)+β H19-C15-C18(24)
50	1023	2.19	49.0	1.45	0.97	ν C6-C5(17)+β H25-N24-C6(51)
51	1022	6.45	3.1	2.20	1.48	ν C33-C35(27)+C32-C35(18)
52	975	1.07	12.8	2.55	1.56	β C1-C2-C3(41)+C5-C4-C3(23)+ C4-C3-C2(14)
53	969	0.57	40.1	2.80	1.69	ν C13-C14(14)
54	966	1.19	6.9	1.47	0.88	τ H36-C32-N39-C30(12)+H37-C33-C35-C32(34)+H38-C35-C33-C31(19)+C31-C33-C35-C32(10)
55	961	4.85	7.7	4.04	2.39	β C31-C33-C35(29)+ N39-C32-C35(11)+C33-C35-C32(13)

56	947	10.90	7.3	1.55	0.89	τ H17-C14-C16-C20(18)+H19-C15-C18-C20(14)+H21-C18-C20-C16(10)+H28-C27-N29-C30(38)
57	943	0.43	3.9	1.33	0.76	τ H7-C1-C6-N24(23)+H8-C2-C1-C6(48)+C1-C2-C3-C4(11)
58	941	0.89	3.0	1.41	0.80	τ H36-C32-N39-C30(42)+H37-C33-C35-C32(17)
59	937	6.83	0.4	1.45	0.82	τ H19-C15-C18-C20(22)+H21-C18-C20-C16(13)+H28-C27-N29-C30(29)+C20-C18-C15-C13(11)
60	925	1.93	16.3	1.33	0.73	τ H9-C4-C5-C6(37)+H10-C5-C6-N24(16)+C5-C4-C3-C2(12)+C6-C5-C4-C3(18)
61	913	7.16	30.2	1.44	0.77	τ H17-C14-C16-C20(49)+H28-C27-N29-C30(11)+C18-C15-C13-C14(10)+Θ C15-C14-N12-C13(14)
62	872	10.18	10.4	5.41	2.64	ν C2-C3(22)+β N11-N12-C13(11)+ C3-N11-N12(10)
63	855	2.79	10.8	1.93	0.90	τ H34-C31-C33-C35(33)+H38-C35-C33-C31(15)
64	844	17.70	46.9	2.95	1.35	ν N29-C30(11)+β C33-C35-C32(17)+τ H34-C31-C33-C35(12)+H38-C35-C33-C31(10)
65	818	61.68	5.3	1.56	0.67	τ H19-C15-C18-C20(24)+H21-C18-C20-C16(33)
66	810	19.28	1.8	1.75	0.74	τ H7-C1-C6-N24(22)+H10-C5-C6-N24(24)
67	804	4.26	10.4	4.50	1.87	ν C4-C3(10)+N24-C6(10)+β C4-C3-C2(23)
68	787	0.13	2.6	1.26	0.50	τ H7-C1-C6-N2(31)+H8-C2-C1-C6(15)+H9-C4-C5-C6(19)+H10-C5-C6-N24(34)
69	785	3.95	18.3	4.68	1.85	β C33-C35-C32(12)
70	771	49.43	51.6	3.38	1.29	τ C30-N39-C32-C35(11)+Θ N29-C31-N39-C30(16)
71	722	22.46	27.0	1.62	0.54	τ H34-C31-C33-C35(25)+H38-C35-C33-C31(28)+C30-N39-C32-C35(28)
72	711	3.42	8.8	4.17	1.35	τ H17-C14-C16-C20(12)+C20-C18-C15-C13(11)+Θ O22-C16-C18-C20(19)+C15-C14-N12-C13(14)
73	697	0.98	1.3	4.15	1.30	τ C1-C2-C3-C4(12)+Θ N24-C5-C1-C6(24)+C4-C2-N11-C3(10)
74	634	5.93	28.7	6.71	1.73	β C20-C18-C15(11)+ C18-C15-C13(19)
75	626	3.36	10.0	6.85	1.72	β C1-C2-C3(12)+C5-C4-C3(27)+ C2-C3-N11(10)+N24-C6-C1(10)
76	610	4.30	6.6	7.05	1.68	β C31-C33-C35(12)+ N39-C32-C35(27)+C30-N39-C32(19)
77	598	7.87	44.0	6.49	1.49	β C20-C18-C15(12)+C6-C5-C4(12)
78	586	3.91	21.8	3.65	0.81	τ H19-C15-C18-C20(10)+C18-C15-C13-

						C14(14)+C13-C14-C16-C27(12)+N12-C13-C14-C16(13)
79	528	14.86	55.5	6.21	1.11	β N11-N12-C13(12)
80	518	7.93	15.5	3.17	0.55	τ C31-C33-H35-H32(11)+Θ C29-C31-H39-H30(22)
81	508	15.79	9.3	2.70	0.45	Θ C24-C5-N1-C6(29)+C4-N2-H11-C3(15)
82	485	16.32	2.5	3.83	0.58	β C29-H30-H39(13)+Θ O22-H16-H18-H20(15)
83	461	41.49	14.3	3.32	0.45	τ H25-C24-C6-C5(12)+N26-C24-C6-C5(12)
84	452	9.85	17.8	4.11	0.54	β N2-C3-H11(10)+ O22-H20-H18(26)
85	440	491.68	27.4	2.15	0.27	τ H25-C24-C6-C5(22)+N26-C24-C6-C5(23)
86	427	6.48	2.1	3.98	0.47	β C29-H30-H39(25)+τ C12-C13-C14-H16(11)
87	415	39.31	0.4	3.07	0.34	τ H9-C4-C5-C6(12)+C5-C4-C3-N2(26)+C6-C5-C4-C3(18)
88	401	3.85	3.7	3.60	0.37	τ H34-C31-C33-H35(10)+H36-H32-H39-H30(12)+H39-H32-H35-C33(19)+H30-H39-H32-H35(11)+C31-C33-C35-C32(36)
89	399	29.92	2.9	4.20	0.43	τ C1-C2-C3-C4(18)+C20-C18-C15-C13(14)+N12-C13-C14-C16(12)+Θ O22-C16-H18-H20(16)
90	385	6.02	6.4	3.31	0.29	β C24-C6-N1(59)
91	368	5.24	14.1	4.69	0.37	τ N1-N2-C3-C4(19)+Θ C4-N2-H11-C3(21)
92	339	13.90	22.5	1.04	0.07	τ H25-C24-C6-C5(47)+N26-C24-C6-C5(47)
93	334	7.32	10.8	4.78	0.31	β C14-N16-C27(12)+O22-H20-H18(10)+τ H39-H32-H35-C33(11)
94	306	94.91	1.9	1.31	0.07	τ H23-O22-H20-H16(77)
95	278	0.57	34.8	5.48	0.25	β N2-C3-H11(13)
96	241	5.89	7.3	3.99	0.14	τ C13-C14-H16-C27(15)
97	225	1.75	2.9	5.72	0.17	τ H39-H32-H35-C33(14)
98	204	1.82	1.6	6.29	0.15	β H11-C12-C13(10)+ N2-C3-H11(10)+τ H39-H32-H35-C33(12)
99	197	1.57	9.9	6.61	0.15	τ H11-C12-C13-C14(11)+N1-N2-C3-C4(10)+C5-C4-C3-N2(10)+N2-C3-H11-C12(26)+C6-C5-C4-C3(25)
100	175	0.22	6.9	3.55	0.06	τ H18-C15-C13-C15(18)
101	130	2.20	2.1	5.52	0.05	β C14-H16-C27(11)+N2-C3-H11(12)
102	116	4.41	0.4	4.46	0.04	τ C27-C29-H30-C31(35)+C13-C14-H16-C27(15)+C14-C16-C27-C29(21)
103	84	0.17	14.0	5.77	0.02	τ C5-C4-C3-N2(17)+H18-C15-C13-C15(16)+N2-C3-H11-C12(24)
104	73	0.44	10.0	5.69	0.02	β C27-C29-H30(19)+ H11-C12-C13(15)+C3-H11-C12(14)+H16-C27-C29(10)
105	57	0.89	2.0	5.05	0.01	τ C27-C29-H30-C31(17)+C13-C14-H16-

						C27(24)+H16-C27-C29-H30(37)
106	42	1.66	5.0	6.40	0.01	τ C3-H11-C12-C13(32)+Θ C15-C14-C12-C13(13)+C4-N2-H11-C3(21)
107	27	1.07	6.9	6.18	0.00	β C27-C29-H30(13)+H11-C12-C13(15)+C14-H16-C27(16)+C3-H11-C12(10)+H16-C27-C29(15)
108	23	3.21	9.2	4.61	0.00	τ C27-C29-H30-C31(18)+C14-H16-C27-C29(55)+H16-C27-C29-H30(11)
109	16	0.20	3.2	3.74	0.00	τ H11-H12-C13-C14(58)+N2-C3-H11-C12(26)

Table No.2: Vibrational wave numbers obtained for compound 2 DFT-B3LYP/6-311+G(d,p) [harmonic frequency (cm^{-1}), IR intensity, Raman activity(Km/mol), reduced masses (amu) and force constants ($mDyneA^{\circ -1}$)]

Mode No	Experimental frequencies cm^{-1} FR IR	Calculated frequencies (cm^{-1})	IR Intensity	Raman activity	Reduced mass	Force constant	Vibrational assignments WITH>10%PED
1	3645	3437	45.7049	413.137	1.0754	8.1046	ν-N11-H12(100)
2	3557	3088	7.1398	65.7688	1.0939	6.6515	ν-C4-H9(65)
3	3422	3085	5.0611	86.4642	1.0932	6.6372	ν-C23-H27(87) + ν-C26-H29(12)
4		3074	4.6806	73.9826	1.0880	6.5585	ν-C4-H9(33)
5		3073	7.1082	375.917	1.0979	6.6171	ν-C36-H39(18)+ν-C40-H43(58) + ν-C38-H42(21)
6		3069	4.7575	95.2752	1.0934	6.5736	ν-C1-H7(11)+ν-C2-H8(84)
7		3067	13.2059	66.6348	1.0922	6.5541	ν-C36-H39(67)+ν-C40-H43(29)
8	3184	3066	7.7190	165.760	1.0892	6.5326	ν-C23-H27(12) + ν-C26-H29(87)
9		3052	13.1538	44.9244	1.0902	6.4779	ν-C22-H25(98)
10	3048	3049	4.4941	102.733	1.0881	6.4531	ν-C38-H42(75) + ν-C36-H39(15)
11	2917	3047	10.4034	131.519	1.0892	6.4526	ν-C1-H7(89)+ν-C2-H8(11)
12		3041	820.62	711.038	1.0707	6.3138	ν-O30-H31(96)
13	2845	3029	52.63	152.699	1.0893	6.3768	ν-C37-H41(94)
14	2726	3023	12.56	94.5579	1.1037	6.4369	ν-C15-H18(68) + ν-C15-H16(32)
15		2992	6.3898	74.8123	1.0966	6.2623	ν-C15-H17(42) + ν-C15-H18(16) + ν-C15-H16(42)
16		2928	2.4129	196.056	1.0387	5.6813	ν-C15-H18(17) + ν-C15-H17(57) + ν-C15-H16(26) + ν-C32-H33(99)
17	2478	1678	780.351	236.609	7.3281	13.162	ν-O14-C13(79)
18	2017	1606	587.446	1789.13	7.1004	11.683	β H33-C32-N34(11) + ν-N34-C32(57)
19	1592	1595	77.6913	605.801	5.6119	9.1139	ν-C22-C24(13)+ν-C28-C26(20) + ν-C21-C22(15)
20	1919	1580	286.022	1868.86	6.0792	9.6811	ν-C1-C2(12)+ν-C5-C4(24) + ν-C2-C3(15)

21	1654	1557	237.141	481.520	4.5991	7.1073	ν-C36-C38(20)
22	1511	1550	90.2754	214.983	6.0234	9.2335	ν-C2-C3(20) + ν-C6-C1(22)
23		1547	117.720	604.115	4.6658	7.1222	ν-C37-C40(22)
24		1538	165.985	1249.24	4.2943	6.4786	ν-C38-C40(11) + β H31-O30-C28(10)
25		1487	21.8989	5409.5	3.8574	5.4368	β H10-C5-C6(11) + ν-N19-N20(33)
26		1466	210.242	3351.76	2.9750	4.0753	β H9-C4-C5(12)+β H29-C26-C23(10)+β H29-C26-C23(10) + ν-N19-N20(11)
27		1442	82.2654	4943.63	2.6818	3.5595	ν-N44-C35(12) + β H41-C37-N44(18)
28		1497	62.4728	306.449	2.1592	2.8476	β H7-C1-C2(10) + β H12-N11-C13(21)
29	1487	1494	79.7101	3452.03	2.3724	3.1166	ν-N19-N20(13)
30		1489	4.7562	610.508	1.2342	1.6103	τ H18-C15-C13-N11(13) + β H16-C15-H18(31)+β H18-C15-H17(24)
31		1479	11.5331	4023.02	2.6391	3.3971	β H41-C37-N44(10) + β H31-O30-C28(18)
32		1477	25.4275	10.0393	1.0549	1.3544	τ H16-C15-C13-N11(10) + β H17-C15-H16(48)+β H16-C15-H18(23)
33		1457	97.8283	116.974	2.1284	2.6584	β H43-C40-C38(29)+β H42-C38-C40(27)
34		1443	87.9837	192.465	2.4220	2.9687	ν-C22-C24(18) + ν-C26-C23(22) + β H31-O30-C28(23)
35		1432	3.0407	1728.8	2.6042	3.1412	ν-C1-C2(14)+ν-C5-C4(20) + β H8-C2-C1(11)+β H10-C5-C6(10) + β H12-N11-C13(18)
36		1404	105.970	50.3173	1.3385	1.5529	β H17-C15-H16(32)+β H18-C15-H17(37)+β H16-C15-H18(14)
37	1399	1387	85.9071	1053.37	2.1492	2.4309	ν-C26-C23(10) + β H33-C32-N34(43)
38	1386	1367	7.4316	261.353	2.7690	3.0425	ν-C21-C22(20) + ν-C28-C26(10) + β H33-C32-N34(12)
39		1338	62.6695	1569.49	4.3387	4.5715	ν-C4-C3(21) + ν-C6-C1(15)
40		1329	24.9396	51.0353	1.7750	1.8431	β H8-C2-C1(11)+β H9-C4-C5(16)+β H10-C5-C6(17)
41		1326	137.289	29.5189	2.4693	2.5545	ν-O30-C28(16)+ν-N11-C13(15)
42		1324	588.721	229.706	2.2604	2.3307	ν-N11-C13(19) + ν-N44-C37(10) + β H41-C37-N44(14)
43		1319	161.013	107.027	2.3215	2.3753	ν-O30-C28(20) + ν-N44-C37(15) + β H41-C37-N44(16) + β H27-C23-C26(10)
44		1296	25.5499	110.169	4.3676	4.3159	ν-C38-C40(11) + ν-N44-C35(26) + ν-N44-C37(16)

45	1276	1279	39.4128	480.589	2.7528	2.6470	ν-N20-C21(15) + β H33-C32-N34(10)
46		1263	81.4285	308.464	3.6184	3.3963	ν-N34-C35(27)
47		1250	48.1170	802.626	2.5698	2.3627	ν-C6-C1(16) + ν-N11-C6(18)
48		1242	29.5619	107.027	2.0770	1.8838	ν-N19-C3(18) + β H25-C22-C24(12)+β H7-C1-C2(15)
49	1202	1224	74.4230	9.3015	2.6589	2.3433	ν-C24-C32(10) + ν-C28-C26(22)
50		1181	189.411	522.91	1.3839	1.1352	β H25-C22-C24(13)+β H9-C4-C5(14)
51		1175	3.6202	6.6041	1.1514	0.9351	ν-C36-C38(11) + ν-C38-C40(11) + β H39-C36-C38(21)+β H43-C40-C38(18)+β H42-C38-C40(36)
52		1165	19.3811	35.1139	1.6175	1.2907	ν-N19-C3(11) + β H8-C2-C1(14)
53	1149	1134	18.4127	120.453	1.2876	0.9740	ν-C1-C2(14) + β H7-C1-C2(11)+β H8-C2-C1(17)+β H9-C4-C5(15)
54		1127	101.504	196.235	1.5108	1.1277	β H27-C23-C26(27)
55	1104	1120	11.5858	83.8249	1.5434	1.1389	ν-C36-C38(15) + ν-C37-C40(13) + β H39-C36-C38(12)+β H43-C40-C38(32)
56		1069	5.2030	35.1139	2.2339	1.5013	ν-C15-C13(29) + ν-C37-C40(20)
57		1056	11.3284	5.1917	1.7376	1.1402	β H16-C15-H18(17) + τ H16-C15-C13-N11(37)+ τ H18-C15-C13-N11(15) + γ O14-C15-N11-C13(19)
58		1004	70.0494	1.6858	1.5849	0.9889	β H17-C15-H16(11)+β H18-C15-H17(11) + τ H16-C15-C13-N11(10)- τ H17-C15-C13-N11(31)- τ H18-C15-C13-N11(11)
59		1030	1.4023	41.4537	2.5066	1.5473	β C5-C4-C3(38)+β C22-C24-C32(15)
60		1025	8.2450	9.3015	1.4721	0.8882	τ H33-C32-N34-C35(44) + τ H43-C40-C38-C36(11)+ τ H42-C38-C40-C37(16)
61		1013	5.1664	10.6792	1.8671	1.1230	β C36-C38-C40(13) + τ H42-C38-C40-C37(17) + τ H33-C32-N34-C35(20)
62	1009	1011	7.0047	195.420	2.9339	1.7386	β C38-C40-C37(12)+β C36-C38-C40(22) + β N44-C37-C40(11) + τ H33-C32-N34-C35(16)
63	966	997	1.3579	17.0606	1.3384	0.7820	τ C28-C26-C23-C21(15)+ τ H27-C23-C26-C28(44)+ τ H29-C26-C28-C24(23)

64		990	0.4708	4.5198	1.3384	0.7714	τ C5-C4-C3-C2(11) + τ H10-C5-C6-N11(25) + τ H9-C4-C5-C6(37)
65		986	1.2676	0.2602	1.4257	0.8144	τ C35-N44-C37-C40(10) + τ H41-C37-N44-C35(50) + τ H42-C38-C40-C37(21)
66		973	0.6198	3.1311	1.3542	0.7536	τ H7-C1-C2-C3(19)+ τ H8-C2-C1-C6(37) + τ C6-C1-C2-C3(17) + β C26-C23-C21(13) + ν-C23-C21(21)
67		928	9.4722	12.8447	5.5132	2.7939	ν-C4-C3(22)
68		924	2.6543	40.082	4.3552	2.1869	β C6-C1-C2(11)
69		919	17.1159	6.8830	1.4589	0.7245	τ H25-C22-C24-C28(63) + γ C23-C22-N20-C21(17)
70		906	34.4496	7.6759	2.9971	1.4464	β C38-C40-C37(12) + τ H39-C36-C38-C40(13)
71		891	27.8608	7.2658	1.1892	0.5544	τ H39-C36-C38-C40(15)+ τ H43-C40-C38-C36(10) + τ H31-O30-C28-C24(53)
72	898	889	38.4352	3.8631	1.5743	0.7322	τ H39-C36-C38-C40(17)+ τ H43-C40-C38-C36(11) + τ H31-O30-C28-C24(24)
73		864	66.8382	3.0003	1.7275	0.7584	τ H7-C1-C2-C3(22)+ τ H8-C2-C1-C6(12)+ τ H9-C4-C5-C6(15) + τ H10-C5-C6-N11(30)
74		854	34.2790	0.4040	1.5496	0.6649	τ H27-C23-C26-C28(24)+ τ H29-C26-C28-C24(33) + τ H31-O30-C28-C24(11)
75	835	834	3.4410	16.338	1.2741	0.5207	τ H7-C1-C2-C3(30)+ τ H8-C2-C1-C6(21)+ τ H9-C4-C5-C6(18) + τ H10-C5-C6-N11(25)
76		824	5.0484	30.185	5.5225	2.2046	ν-C2-C3(11)
77		815	33.6406	10.391	3.0231	1.1790	τ H43-C40-C38-C36(11) + γ N34-C40-C38-C36(17)
78		793	1.8674	10.7864	4.1810	1.5467	ν-C15-C13(25)
79		756	23.8083	5.2521	1.6226	0.5445	τ C35-N44-C37-C40(25) + τ H39-C36-C38-C40(26) + τ H43-C40-C38-C36(28)
80		747	2.2126	1.8154	4.1991	1.3773	τ H25-C22-C24-C28(12)+ τ H29-C26-C28-C24(11) + γ O30-C24-C26-C28(25) + γ C23-C22-N20-C21(13)
81	739	738	1.1786	10.4024	4.3047	1.3769	τ C5-C4-C3-C2(14)+ τ C6-C1-C2-C3(11) + γ N11-C5-C1-C6(13)
82		714	18.2621	2.6474	5.8495	1.7536	β C24-C32-N34(10)
83	672	668	28.4039	18.2995	4.6587	1.2216	β C26-C23-C21(10)
84		655	82.2850	51.6104	2.1347	0.5378	τ H12-N11-C13-C15(29) + τ H18-C15-C13-N11(10) + γ

							O14-C15-N11-C13(31)
85		652	14.3190	27.0134	4.9305	1.2293	β C1-C2-C3(21)+β C5-C4-C3(13)+β C6-C1-C2(13)
86		640	4.0581	8.8273	7.0531	1.6962	β C36-C38-C40(15) + β N44-C37-C40(33) + β C35-N44-C37(22)
87		612	6.7771	1.3130	3.1687	0.6963	τ C26-C23-C21-C22(11)+ τ C21-C22-C24-C32(15) + τ C3-N19-N20-C21(10) + τ H27-C23-C26-C28(12)
88		591	13.1355	28.7106	7.6556	1.5715	β O30-C28-C26(10) + β C35-N44-C37(13)
89		574	11.1412	9.9645	4.5767	0.8855	β C22-C24-C32(10) + β C23-C21-N20(10)
90		561	19.4963	6.6108	3.2849	0.6067	β O14-C13-C15(15)
91		545	38.1349	43.9857	2.8478	0.4971	τ H12-N11-C13-C15(12) + β O14-C13-C15(13)
92		540	4.5808	21.8493	3.4658	0.5931	β C3-N19-N20(11)
93		526	41.1288	55.4532	2.0266	0.3296	τ H18-C15-C13-N11(11) + τ H12-N11-C13-C15(28) + γ O14-C15-N11C13(19)
94		511	2.7081	15.4961	3.3565	0.5151	β N34-C35-N44(18)+β N34-C35-N44(18) + β O14-C13-C15(23) + γ C4-C2-N19-C3(10)
95		465	7.8622	2.5491	3.7454	0.4755	τ N20-C21-C22-C24(31) + γ O30-C24-C26-C28
96		448	3.9887	14.3363	5.3179	0.6249	β C28-C26-C23(10)+β C28-C26-C23(10) + β O30-C28-C26(48)
97		433	3.5857	17.7924	3.5350	0.3890	τ C6-C1-C2-C3(27) + τ C1-C2-C3-N19(14) + γ N11-C5-C1-C6(11)
98		423	2.8162	27.4328	3.5900	0.3766	τ H39-C36-C38-C40(11) + τ N44-C37-C40-C38(16) + τ H41-C37-N44-C35(12) + τ C35-N44-C37-C40(13) + τ C36-C38-C40-C37(36)
99		417	3.0020	2.0667	4.4850	0.4576	τ C5-C4-C3-C2(28)
100		396	42.8284	0.3852	8.1970	0.7585	ν-N11-C6(17)
101		374	5.7933	3.6804	5.4125	0.4461	τ C28-C26-C23-C21(15)
102		360	5.2519	2.9131	4.7136	0.3604	β C15-C13-N11(18) + τ C28-C26-C23-C21(11)
103		337	5.7925	6.4034	4.7057	0.3155	β C15-C13-N11(12)
104		324	4.1785	14.0584	3.6558	0.2257	τ C22-C24-C32-N34(17) + τ C21-C22-C24-C32(18)
105		274	0.3313	22.4594	5.4352	0.2409	τ N44-C37-C40-C38(17)
106		239	0.9230	10.7723	5.0947	0.1713	β C13-N11-C6(21)
107		213	0.5021	1.8832	6.3042	0.1690	β C23-C21-N20(16)+β C24-

							C32-N34(13)
108		201	2.6857	34.7749	5.9604	0.1415	τ N19-N20-C21-C22(19) + τ C22-C24-C32-N34(24) + τ C32-N34-C35-C36(10)
109		187	2.8942	7.2685	2.9873	0.0625	τ H17-C15-C13-N11(25)+ τ H16-C15-C13-N11(18)
110		188	1.1928	2.9059	1.3170	0.0272	β C22-C24-C32(15) + τ N44-C37-C40-C38(10)
111		169	1.2082	1.5560	7.9716	0.1338	ν-N20-C21(10)
112		131	3.2384	9.9088	5.5862	0.0693	τ C22-C24-C32-N34(13) + τ C26-C23-C21-C22(19)+ τ C21-C22-C24-C32(16)
113		145	4.1828	6.9466	5.4533	0.0552	β C13-N11-C6(17)
114		95	5.7668	2.1384	6.9422	0.0365	τ C15-C13-N11-C6(12) + τ C2-C3-N19-N20(11)+ τ C13-N11-C6-C5(17)
115		75	1.8709	0.4273	6.0950	0.0203	τ C15-C13-N11-C6(11) + β C32-N34-C35(11)
116		63	0.1384	14.0135	6.5759	0.0154	τ C13-N11-C6-C5(24) + β C32-N34-C35(13)
117		54	5.5134	9.9864	3.9561	0.0070	τ C15-C13-N11-C6(17) + τ C13-N11-C6-C5(23)
118		52	1.7367	2.0024	5.0359	0.0080	τ C24-C32-N34-C35(29)+ τ C15-C13-N11-C6(13) + τ C2-C3-N19-N20(10) + τ C21-C22-C24-C32(17)
119		37	0.2603	5.0249	5.4234	0.0043	τ C32-N34-C35-C36(32) + τ C1-C2-C3-N19(14)+ τ C22-C24-C32-N34(11)
120		28	0.5720	6.9310	5.8738	0.0028	β C32-N34-C35(10) + β N19-N20-C21(16) + β N19-N20-C21(16) + β C3-N19-N20(17)
121		23	1.7957	9.2389	5.4983	0.0018	τ C32-N34-C35-C36(23) + τ C22-C24-C32-N34(12)+ τ C1-C2-C3-N19(12) + τ C3-N19-N20-C21(17)
122		19	0.1501	3.1535	4.3806	0.0010	τ C2-C3-N19-N20(35) + τ N19-N20-C21-C22(33)

Table No.3: Mulliken atomic charges and natural population analysis by B3LYP/6-311+G(d,p) methods for compounds 1 and 2

S.No	Atoms	Mulliken atomic charge 1	NPA 1	Atoms	Mulliken atomic charge 2	NPA 2
1	C1	-0.2541	-0.2480	C1	-0.3314	-0.2261
2	C2	0.0666	-0.1657	C2	0.0771	-0.1604
3	C3	-0.3309	0.0579	C3	-0.5839	0.086
4	C4	0.0461	-0.1464	C4	-0.1682	-0.1771
5	C5	-0.0237	-0.2627	C5	0.3015	-0.2254
6	C6	-0.1280	0.1879	C6	0.0726	0.1661
7	H7	0.1070	0.2028	H7	0.1248	0.2121
8	H8	0.1488	0.2281	H8	0.1347	0.2221
9	H9	0.1344	0.2209	H9	0.1506	0.2304
10	H10	0.1079	0.2050	H10	0.1239	0.2127
11	N11	0.0452	-0.2041	N11	-0.1959	-0.6302
12	N12	0.0664	-0.2334	H12	0.2815	0.4037
13	C13	-0.5611	0.0735	C13	0.0877	0.6874
14	C14	-0.3871	-0.1283	O14	-0.3168	-0.6111
15	C15	0.1176	-0.1405	C15	-0.3882	-0.6727
16	C16	1.1729	-0.1834	H16	0.1658	0.2202
17	H17	0.1890	0.2194	H17	0.1711	0.2256
18	C18	0.3938	-0.2574	H18	0.1805	0.236
19	H19	0.1356	0.7800	N19	0.119	-0.2267
20	C20	-1.7930	0.359	N20	0.0337	-0.2321
21	H21	0.1319	0.2233	C21	-0.6821	0.1577
22	O22	-0.2067	-0.6676	C22	-0.8865	-0.1570
23	H23	0.2396	0.4731	C23	0.2856	-0.1788
24	N24	-0.3613	-0.7791	C24	0.9511	-0.2008
25	H25	0.2330	0.3787	H25	0.1242	0.2214
26	H26	0.2334	0.379	C26	-0.2799	-0.2467
27	C27	0.3091	0.1396	H27	0.1575	0.2319
28	H28	0.0619	0.1327	C28	-0.0986	0.4005
29	N29	0.2290	-0.4224	H29	0.1399	0.2219
30	C30	-0.5084	0.3617	O30	-0.3343	-0.6614
31	C31	0.3948	-0.2708	H31	0.428	0.5123
32	C32	-0.2051	0.0636	C32	0.1477	0.1669
33	C33	-0.2941	-0.1608	H33	0.1096	0.1715
34	H34	0.1330	0.2149	N34	0.0204	-0.5228
35	C35	0.0382	-0.2615	C35	-0.4890	0.368
36	H36	0.1317	0.1888	C36	0.4314	-0.2620
37	H37	0.1344	0.2099	C37	-0.2075	0.0646
38	H38	0.1309	0.2137	C38	-0.3598	-0.1585
39	N39	-0.0787	-0.4546	H39	0.1314	0.2152
40				C40	0.0435	-0.2526
41				H41	0.1351	0.1914
42				H42	0.1377	0.212
43				H43	0.1345	0.2158
44				N44	-0.0801	-0.4509

Table No.4: The *ab initio* and DFT calculated electric dipole moment (Debye), average polarizability (α_{tot} x 10^{24}esu) and hyperpolarizability (β_{tot} x 10^{30}esu) for compounds 1 and 2

S.No	Parameters	DFT /6-311G+(d,p) 1	DFT /6-311G+(d,p) 2
Dipole moment			
1	μ_x	0.74	-3.12
2	μ_y	-0.75	-2.75
3	μ_z	2.49	-0.95
4	μ	2.70	4.3
Polarizability			
5	α_{xx}	38.33	-24.65
6	α_{YY}	-11.48	19.58
7	α_{ZZ}	-26.85	5.06
8	α_{XY}	-6.68	37.01
9	α_{XZ}	0.72	9.92
10	α_{yz}	-4.12	0.35
11	α_0	1.2E-15	3.3E-05
12	α_{tot}	1E-23	1E-23
Hyperpolarizability			
13	β_{xxx}	171.57	-682.45
14	β_{yyy}	-37.44	-11.39
15	β_{zzz}	5.19	1.96
16	β_{xyy}	45.27	-5.39
17	β_{xxy}	-121.98	-10.19
18	β_{xxz}	93.52	-7.31
19	β_{xzz}	-25.39	15.63
20	β_{yzz}	2.17	-10.97
21	β_{yyz}	-0.32	-6.41
22	β_{xyz}	-11.09	-29.59
23	β_{tot}	266	673
24	β_0	2.3	5.8

Table No.5: HOMO and LUMO energy, chemical potential, hardness and electrophilicity index calculated by B3LYP/6-311G (d, p) method for compounds 1 and 2

S.No	Method	B3LYP/6311+G(d,p) 1	B3LYP/6311+G(d,p) 2
1	E_{HOMO} (eV)	-5.6453	-6.1217
2	E_{LUMO} (eV)	-2.2296	-2.3575
3	$\Delta E=E_{HOMO}-E_{LUMO}$(eV)	1.7079	1.8821
4	Electronegativity ($\mu= -\chi$)	3.9375	4.2396
5	Hardness (η)	1.7079	1.8821
6	Electrophilicity index (ω)	2.2695	2.3875

Table No.6: Theoretically computed energies (a.u), zero-point vibrational energy (kcal/mol), rotational constants (Ghz), entropy (cal $mol^{-1}K^{-1}$) and dipole moment (Debye) for 1 and 2

S.No	Parameters	DFT-B3LYP/ 6-311+G(d,p) 1	DFT-B3LYP/ 6-311+G(d,p) 2
1	Total Energies	-1044.2	-1196.9
2	Zero point energy	188.3	212.9
3	Rotational constants		
4		0.3383	0.4701
5		0.0934	0.048
6		0.0746	0.0441
7	Entropy		
8	Total	155.3	167.8
9	Translational	43.16	43.5
10	Rotational	36.17	37.0
11	Vibrational	75.95	87.3
12	Dipole moment(D)	2.71	4.3

Table No.S1: Geometric bond lengths (Å), bond angles and dihedral angles (°) of compound 1 DFT-B3LYP/6-311+G(d,p)

S.No	Bond length	B3LYP/6-311+G(d,p)	Bond angle	B3LYP/6-311+G(d,p)	Dihedral angle	B3LYP/6-311+G(d,p)
1	C1-C2	1.3814	C14-C13-C15	119.1	C4-C5-C6-N24	-177.7
2	C1-C6	1.4105	C13-C14-C16	121.2	H10-C5-C6-C1	179.6
3	C1-H7	1.0857	C13-C14-H17	120.0	H10-C5-C6-N24	2.1
4	C2-C3	1.4065	C16-C14-H17	118.8	C1-C6-N24-H25	21.2
5	C2-H8	1.0823	C13-C15-C18	120.8	C1-C6-N24-H26	161.8
6	C3-C4	1.4011	C13-C15-H19	118.5	C5-C6-N24-H25	-161.4
7	C3-N11	1.4059	C18-C15-H19	120.7	C5-C6-N24-H26	-20.8
8	C4-C5	1.3858	C14-C16-C20	118.7	C3-N11-N12-C13	179.9
9	C4-H9	1.0838	C14-C16-C27	119.9	N11-N12-C13-C14	0.3
10	C5-C6	1.4044	C20-C16-C27	121.3	N11-N12-C13-C15	-179.8
11	C5-H10	1.0851	C15-C18-C20	120.1	N12-C13-C14-C16	179.8
12	C6-N24	1.3862	C15-C18-H21	121.5	N12-C13-C14-H17	0.1
13	N11-N12	1.2563	C20-C18-H21	118.5	C15-C13-C14-C16	0.0
14	N12-C13	1.4164	C16-C20-C18	120.2	C15-C13-C14-H17	-179.7
15	C13-C14	1.3933	C16-C20-O22	124.0	N12-C13-C15-C18	179.6
16	C13-C15	1.4045	C18-C20-O22	115.8	N12-C13-C15-H19	0.0
17	C14-C16	1.4012	C20-O22-H23	111.2	C14-C13-C15-C18	-0.5
18	C14-H17	1.0817	C6-N24-H25	117.2	C14-C13-C15-H19	179.9
19	C15-C18	1.3836	C6-N24-H26	117.2	C13-C14-C16-C20	0.8
20	C15-H19	1.0837	H25-N24-H26	113.7	C13-C14-C16-C27	-178.3
21	C16-C20	1.4149	C16-C27-H28	117.5	H17-C14-C16-C20	-179.4
22	C16-C27	1.4656	C16-C27-N29	123.2	H17-C14-C16-C27	1.5
23	C18-C20	1.3967	H28-C27-N29	119.3	C13-C15-C18-C20	0.2
24	C18-H21	1.0829	C27-N29-C30	119.9	C13-C15-C18-H21	-179.3

25	C20-O22	1.3652	N29-C30-C31	121.4	H19-C15-C18-C20	179.8
26	O22-H23	0.9621	N29-C30-N39	115.9	H19-C15-C18-H21	0.3
27	N24-H25	1.0082	C31-C30-N39	122.6	C14-C16-C20-C18	-1.2
28	N24-H26	1.0082	C30-C31-C33	118.6	C14-C16-C20-O22	179.0
29	C27-H28	1.1017	C30-C31-H34	120.3	C27-C16-C20-C18	177.9
30	C27-N29	1.275	C33-C31-H34	121.1	C27-C16-C20-O22	-2.0
31	N29-C30	1.4019	C35-C32-H36	120.3	C14-C16-C27-H28	172.6
32	C30-C31	1.4059	C35-C32-N39	124.0	C14-C16-C27-N29	-7.0
33	C30-N39	1.3384	H36-C32-N39	115.7	C20-C16-C27-H28	-6.4
34	C31-C33	1.3894	C31-C33-C35	119.0	C20-C16-C27-N29	173.9
35	C31-H34	1.0832	C31-C33-H37	120.2	C15-C18-C20-C16	0.7
36	C32-C35	1.3941	C35-C33-H37	120.8	C15-C18-C20-O22	-179.4
37	C32-H36	1.0868	C32-C35-C33	117.9	H21-C18-C20-C16	-179.9
38	C32-N39	1.3336	C32-C35-H38	120.5	H21-C18-C20-O22	0.0
39	C33-C35	1.3922	C33-C35-H38	121.6	C16-C20-O22-H23	-7.9
40	C33-H37	1.0845	C30-N39-C32	117.9	C18-C20-O22-H23	172.2
41	C35-H38	1.0831	Dihedral angle	B3LYP/6-311+G(d,p)	C16-C27-N29-C30	175.7
42	Bond angle	B3LYP/6-311+G(d,p)	C6-C1-C2-C3	-0.1	H28-C27-N29-C30	-4.0
43	C2-C1-C6	120.9	C6-C1-C2-H8	179.9	C27-N29-C30-C31	-52.0
44	C2-C1-H7	119.9	H7-C1-C2-C3	179.7	C27-N29-C30-N39	131.1
45	C6-C1-H7	119.2	H7-C1-C2-H8	-0.3	N29-C30-C31-C33	-177.8
46	C1-C2-C3	120.4	C2-C1-C6-C5	0.2	N29-C30-C31-H34	0.1
47	C1-C2-H8	120.7	C2-C1-C6-N24	177.7	N39-C30-C31-C33	-1.1
48	C3-C2-H8	119.0	H7-C1-C6-C5	-179.6	N39-C30-C31-H34	176.9
49	C2-C3-C4	118.8	H7-C1-C6-N24	-2.1	N29-C30-N39-C32	178.7
50	C2-C3N11	125.2	C1-C2-C3-C4	0.0	C31-C30-N39-C32	1.8
51	C4-C3-N11	116.0	C1-C2-C3-N11	180.0	C30-C31-C33-C35	-0.2
52	C3-C4-C5	121.0	H8-C2-C3-C4	-180.0	C30-C31-C33-H37	179.4
53	C3-C4-H9	118.3	H8-C2-C3-N11	0.0	H34-C31-C33-C35	-178.1
54	C5-C4-H9	120.7	C2-C3-C4-C5	0.0	H34-C31-C33-H37	1.5
55	C4-C5-C6	120.3	C2-C3-C4-H9	-180.0	H36-C32-C35-C33	179.6
56	C4-C5-H10	120.1	N11-C3-C4-C5	-180.0	H36-C32-C35-H38	0.4
57	C6-C5-H10	119.7	N11-C3-C4-H9	0.1	N39-C32-C35-C33	0.2
58	C1-C6-C5	118.7	C2-C3-N11-N12	0.4	N39-C32-C35-H38	-179.1
59	C1-C6-N24	120.4	C4-C3-N11-N12	-179.7	C35-C32-N39-C30	-1.4
60	C5-C6-N24	120.9	C3-C4-C5-C6	0.1	H36-C32-N39-C30	179.2
61	C3-N11-N12	116.0	C3-C4-C5-H10	-179.7	C31-C33-C35-C32	0.6
62	N11-N12-C13	115.1	H9-C4-C5-C6	-179.9	C31-C33-C35-H38	179.8
63	N12-C13-C14	125.1	H9-C4-C5-H10	0.3	H37-C33-C35-C32	-179.0
64	N12-C13-C15	115.8	C4-C5-C6-C1	-0.2	H37-C33-C35-H38	0.2

Table No.S2: Geometric bond lengths (Å), bond angles and dihedral angles (°) of compound 2 DFT-B3LYP/6-311+G(d,p)

S.No	Bond lengths	B3LYP/6-311+G(d,p)	Bond angles	B3LYP/6-311+G(d,p)	Bond angles	B3LYP/6-311+G(d,p)	Dihedral angles	B3LYP/6-311+G(d,p)
1	C1-C2	1.3873	C2-C3-N19	116.0	C40-C37-H41	0.7	N20-C21-C22-C24	-179.9
2	C1-C16	1.4015	C4-C3-N19	125.0	C40-C37-N44	179.9	N20-C21-C22-H25	0.0
3	C1-H7	1.0846	C3-C4-C5	120.4	H41-C37-N44	-178.6	C23-C21-C22-C24	0.1
4	C2-C3	1.3995	C3-C4-H9	119.1	C36-C38-C40	0.5	C23-C21-C22-H25	-179.9
5	C2-H8	1.0835	C5-C4-H9	120.5	C36-C38-H42	0.9	N20-C21-C23-C26	-179.8
6	C3-C4	1.4032	C4-C5-C6	120.6	C40-C38-H42	177.9	N20-C21-C23-H27	0.1
7	C3-N19	1.4134	C4-C5-H10	119.4	C37-C40-C38	-179.8	C22-C21-C23-C26	0.1
8	C4-C5	1.3855	C6-C5-H10	119.9	C37-C40-H43	-2.7	C22-C21-C23-H27	180.0
9	C4-H9	1.0821	C1-C6-C5	118.9	C38-C40-H43	-1.3	C21-C22-C24-C28	-0.4
10	C5-C6	1.4048	C1-C6-N11	118.5	C35-N44-C37	179.4	C21-C22-C24-C32	180.0
11	C5-H10	1.0817	C5-C6-N11	122.5	Dihedral angles	179.5	H25-C22-C24-C28	179.7
12	C6-N11	1.4101	C6-N11-H12	116.3	C6-C1-C2-C3	0.3	H25-C22-C24-C32	0.0
13	N11-H12	1.0125	C6-N11-C13	131.9	C6-C1-C2-H8	0.2	C21-C23-C26-C28	-0.1
14	N11-C13	1.3868	H12-N11-C13	111.5	H7-C1-C2-C3	-178.3	C21-C23-C26-H29	179.8
15	C13-O14	1.2185	N11-C13-O14	119.1	H7-C1-C2-H8	179.4	H27-C23-C26-C28	180.0
16	C13-C15	1.5136	N11-C13-C15	119.1	C2-C1-C6-C5	0.9	H27-C23-C26-H29	-0.1
17	C15-H16	1.0904	O14-C13-C15	121.8	C2-C1-C6-N11	-178.4	C22-C24-C28-C26	0.3
18	C15-H17	1.0935	C13-C15-H16	113.2	H7-C1-C6-C5	2.4	C22-C24-C28-O30	-179.5
19	C15-H18	1.089	C13-C15-H17	109.9	H7-C1-C6-N11	1.4	C32-C24-C28-C26	180.0
20	N19-N20	1.256	C13-C15-H18	107.3	C1-C2-C3-C4	-176.8	C32-C24-C28-O30	0.2
21	N20-C21	1.4093	H16-C15-H17	108.4	C1-C2-C3-N19	179.9	C22-C24-C32-H33	1.6
22	C21-C22	1.3903	H16-C15-H18	110.2	H8-C2-C3-C4	1.6	C22-C24-C32-N34	-179.6
23	C21-C23	1.413	H17-C15-H18	107.8	H8-C2-C3-N19	-1.9	C28-C24-C32-H33	-178.1
24	C22-	1.4022	C3-N19-N20	115.4	C2-C3-C4-C5	-178.8	C28-C24-	0.7

	C24						C32-N34	
25	C22-H25	1.085	N19-N20-C21	115.5	C2-C3-C4-H9	176.3	C23-C26-C28-C24	-0.1
26	C23-C26	1.3783	N20-C21-C22	116.1	N19-C3-C4-C5	-0.6	C23-C26-C28-O30	179.7
27	C23-H27	1.0823	N20-C21-C23	124.9	N19-C3-C4-H9	-31.0	H29-C26-C28-C24	180.0
28	C24-C28	1.4224	C22-C21-C23	119.0	C2-C3-N19-N20	141.3	H29-C26-C28-O30	-0.2
29	C24-C32	1.4492	C21-C22-C24	121.5	C4-C3-N19-N20	145.9	C24-C28-O30-H31	0.8
30	C26-C28	1.4074	C21-C22-H25	118.5	C3-C4-C5-C6	-41.8	C26-C28-O30-H31	-179.0
31	C26-H29	1.0834	C24-C22-H25	120.0	C3-C4-C5-H10	-179.9	C24-C32-N34-C35	177.8
32	C28-O30	1.3325	C21-C23-C26	120.6	H9-C4-C5-C6	-1.1	H33-C32-N34-C35	-3.4
33	O30-H31	0.9963	C21-C23-CH27	118.7	H9-4C-C5-H10	-7.3	H33-C32-N34-C36	-41.7
34	C32-H33	1.0964	C26-C23-H27	120.7	C4-C5-C6-C1	171.5	C32-N34-C35-N44	140.9
35	C32-N34	1.2865	C22-C24-C28	118.8	C4-C5-C6-N11	-31.4	N34-C35-C36-C38	-178.9
36	N34-C35	1.4064	C22-C24-C32	120.0	H10-C5-C6-C1	89.9	N34-C35-C36-H39	-0.8
37	C35-C36	1.404	C28-C24-C32	121.1	H10-C5-C6-N11	-153.1	N44-C35-C36-C38	-1.8
38	C35-N44	1.3369	C23-C26-C28	120.7	C1-C6-N11-H12	147.4	N44-C35-C36-H39	176.4
39	C36-C38	1.3892	C23-C26-H29	121.3	C1-C6-N11-C13	-91.3	N34-C35-N44-C37	179.5
40	C36-H39	1.083	C28-C26-H29	118.0	C5-C6-N11-H12	25.7	C36-C35-N44-C37	2.2
41	C37-C40	1.3937	C24-C28-C26	119.4	C5-C6-N11-C13	-179.8	C35-C36-C38-C40	0.3
42	C37-H41	1.0864	C24-C28-O30	122.2	C6-N11-C13-O14	-179.8	C35-C36-C38-H42	179.6
43	C37-N44	1.3338	C26-C28-O30	118.4	C6-N11-C13-C15	0.2	H39-C36-C38-C40	-177.9
44	C38-C40	1.3923	C28-O30-H31	108.1	H12-N11-C13-O14	0.7	H39-C36-C38-H42	1.5
45	C38-H42	1.0843	C24-C32-H33	116.6	H12-N11-C13-C15	179.9	H41-C37-C40-C38	179.1
46	C40-H43	1.083	C24-C32-N34	121.9	N11-C13-C15-H16	-178.6	H41-C37-C40-H43	0.1
47	Bond angles	B3LYP/6-311+G(d,p)	H33-C32-N34	121.4	N11-C13-C15-H17	0.5	N44-C37-C40-C38	-0.3
48	C2-C1-C6	120.4	C32-N24-C35	121.2	N11-C13-C15-H18	0.9	N44-C37-C40-H43	-179.4
49	C2-C1-H7	120.1	N34-C35-C36	122.0	O14-C13-C15-H16	177.9	C40-C37-N44-C35	-1.1

50	C6-C1-H7	119.5	N34-C35-N44	115.2	O14-C13-C15-H17	-179.8	H41-C37-N44-C35	179.4
51	C1-C2-C3	120.6	C36-C35-N44	122.7	O14-C13-C15-H18	-2.7	C36-C38-C40-C37	0.7
52	C1-C2-H8	120.8	C35-C36-C38	118.5	C3-N19-N20-C21	-1.3	C36-C38-C40-H43	179.7
53	C3-C2-H8	118.6	C35-C36-H39	120.6	N19-N20-C21-C22	179.4	H42-C38-C40-C37	-178.6
54	C2-C3-C4	119.0	C38-C36-H39	120.9	N19-N20-C21-C23	179.5	H42-C38-C40-H43	0.4

Table No.S3: Second order perturbation theory analysis of Fock matrix in NBO basis for compound 1 using B3LYP/6-311+G (d, p) method

S.No	Donor	Occupancy	Acceptor	$E^{(2)}$ kcal/mol	$E_{(j)}$-$E_{(i)}$ a.u.	F(i,j) a.u.
1	π- C1 - C2	1.7293	π*-C3 - C4	14.96	0.29	0.061
2	π-C1 - C2	1.7293	π*-C5 - C6	21.94	0.28	0.072
3	π- C3 - C4	1.6083	π*- C5 - C6	17.56	0.27	0.061
4	π-C3 -C4	1.6083	π*-N11 - N12	23.67	0.23	0.068
5	π-C5-C6	1.6185	π*-C1 - C2	14.19	0.29	0.059
6	π-C5-C6	1.6185	π*-C3 - C4	25.77	0.29	0.077
7	π-C13 -C14	1.6176	π*- N11 - N12	15.32	0.24	0.056
8	π-C13-C14	1.6176	π*-C15 - C18	22.2	0.28	0.072
9	π-C13 - C14	1.6176	π*- C16 - C20	17.57	0.26	0.062
10	π-C15 - C18	1.6920	π*- C13 - C14	15.34	0.3	0.061
11	π- C15 - C18	1.6920	π*-C16 - C20	23.74	0.27	0.074
12	π-C16 - C20	1.6020	π*-C13 - C14	22.11	0.3	0.074
13	π- C16 - C20	1.6020	π*-C15 - C18	14.47	0.29	0.06
14	π- C16 - C20	1.6020	π*- C27 - N29	18.88	0.29	0.07
15	π- C30 - N39	1.6912	π*- C31 - C33	12.29	0.32	0.056
16	π- C30 - N39	1.6912	π*- C32 - C35	28.28	0.32	0.085
17	π- C31 - C33	1.6912	π*- C30 - N39	27.16	0.27	0.079
18	π- C31 - C33	1.6912	π*- C32 - C35	16.27	0.29	0.061
19	π- C32 - C35	1.6376	π*- C30 - N39	16.1	0.27	0.059
20	π-C32 - C35	1.6376	π*- C31 - C33	24.2	0.28	0.074
21	LP (2) O22	1.8209	π*-C16 - C20	28.25	0.35	0.097
22	LP (1) N24	1.8209	π*-C5 - C6	30.25	0.32	0.093
23	LP (1) N29	1.8583	π*-C27 - H28	12.66	0.71	0.087
24	LP (1) N29	1.8583	π*-C30 - N39	10.24	0.35	0.058
25	LP (1) N39	1.9104	π*-C30 - C31	10.23	0.88	0.086
26	π*-C5 - C6	0.4056	π*- C1 - C2	247.28	0.01	0.081
27	π*-C5 - C6	0.4056	π*- C3 - C4	322.73	0.01	0.082
28	π*-N11 - N12	0.2427	π*- C3 - C4	31.4	0.05	0.061
29	π*-N11 - N12	0.2427	π*-C13 - C14	32.89	0.05	0.067
30	π*- C16 - C20	0.4408	π*- C13 - C14	133.05	0.02	0.081
31	π*-C16 - C20	0.4408	π*-C15 - C18	192.21	0.02	0.082
32	π*-C30 - N39	0.4227	π*- C27 - N29	45.77	0.02	0.046
33	π*- C30 - N39	0.4227	π*- C31 - C33	255.67	0.01	0.083
34	π*-C30 - N39	0.4227	π*- C32 - C35	187.02	0.02	0.08

Table No.S4: Second order perturbation theory analysis of Fock matrix in NBO basis for compound 2 using B3LYP/6-311+G (d, p) method

S.No	Donor	Occupancy	Acceptor	$E^{(2)}$ kcal/mol	E_j-E_i a.u	F(i,j) a.u
1	π-C1 -C6	1.6417	π*-C2-C3	22.14	0.29	0.072
2	π-C1 -C6	1.6417	π*-C4-C5	16.73	0.29	0.064
3	π-C1 -C6	1.6417	σ*-N11-H12	0.79	0.66	0.022
4	π-C1 -C6	1.6417	σ*-N11-C13	1.32	0.7	0.029
5	π-C2-C3	1.6072	π*-C1-C6	19.9	0.27	0.066
6	π-C2-C3	1.6072	π*-C4-C5	20.57	0.28	0.07
7	π-C2-C3	1.6072	π*-N19-N20	20.82	0.23	0.064
8	π-C4-C5	1.6962	π*-C1-C6	21.23	0.28	0.07
9	π-C4 -C5	1.6962	π*-C2-C3	17.29	0.29	0.064
10	π-N19-N20	1.9144	π*-C2-C3	10.4	0.39	0.062
11	π-N19-N20	1.9144	π*-C21-C22	9.37	0.39	0.058
12	π-C21-C22	1.6327	π*-N19-N20	22.77	0.23	0.067
13	π-C21-C22	1.6327	π*-C23-C26	20.55	0.29	0.07
14	π-C23-C26	1.7145	π*-C21-C22	13.98	0.29	0.057
15	π-C32-N34	1.9135	σ*-C35-C36	1.5	0.89	0.033
16	π-C32-N34	1.9135	σ*-C35-N44	1.77	0.88	0.036
17	π-C32-N34	1.9135	π*-C35-N44	10.16	0.35	0.059
18	π-C35-N44	1.6942	σ*-C32-N34	0.51	0.9	0.021
19	π-C35-N44	1.6942	π*-C36-C38	12.5	0.32	0.056
20	π-C35-N44	1.6942	π*-C37-C40	24.73	0.35	0.083
21	π-C35-N44	1.6942	σ*-C37-H41	0.99	4.08	0.061
22	π-C36-C38	1.6695	π*-C35-N44	27.25	0.27	0.079
23	π-C36-C38	1.6695	π*-C37-C40	14.98	0.32	0.062
24	π-C37-C40	1.6321	π*-C35-N44	15.91	0.27	0.059
25	π-C37-C40	1.6321	π*-C36-C38	23.82	0.28	0.074
26	π-C37 -C40	1.6321	σ*-C38-H42	0.74	3.39	0.049
27	LP(1)N11	1.6859	π*-C1 -C6	23.64	0.28	0.074
28	LP(1)N11	1.6859	π*-C13-O14	51.86	0.29	0.111
29	LP(1)O14	1.9784	σ*-N11-C13	1.24	1.12	0.034
30	LP(2)O14	1.8691	σ*-C6-N11	0.54	0.67	0.017
31	LP(1)N19	1.9526	σ*-C2-C3	0.67	0.96	0.023
32	LP(1)N19	1.9526	σ*-C21-C22	0.79	0.97	0.025
33	LP(1)N19	1.9526	σ*-C23-C26	0.51	1	0.02
34	LP(1)N20	1.9520	σ*-C2-C3	0.96	0.97	0.027
35	LP(1)N20	1.9520	σ*-C21-C22	0.52	0.97	0.02
36	LP(1)C24	1.1072	π*-C21-C22	70.81	0.15	0.108
37	LP(1)C24	1.1072	π*-C32-N34	61.85	0.14	0.101
38	LP(1)O30	1.9728	σ*-C24-C28	6.92	1.09	0.078
39	LP(1)O30	1.9728	σ*-C26-C28	0.63	1.11	0.024
40	LP(1)N34	1.8451	σ*-C35-N44	1.56	0.9	0.035
41	LP(1)N34	1.8451	π*-C35-N44	6.39	0.37	0.047
42	LP(1)N44	1.9104	σ*-C37-C40	8.7	0.9	0.08
43	LP(1)N44	1.9104	σ*-C37-H41	0.95	4.12	0.057
44	LP(1)N44	1.9104	σ*-C38-C40	1.43	3.33	0.063
45	LP(1)N44	1.9104	σ*-C38-H42	1.27	3.46	0.06

Table No.S5: DFT-B3LYP/6-311+G (d, p) method calculated NICS (ppm) values (neutral, cation and anion) compound 2

S.No	Bq	NICS (Anilide ring)					
		Neutral isotropic	Neutral anisotrpic (zz)	Cation isotropic	Cation anisotropic (zz)	Anion isotropic	Anion aniotropic (zz)
1	-2	-4.9105	-16.417	-4.0964	-12.0861	-3.8934	-13.386
2	-1.5	-7.3672	-21.596	-6.4089	- 13.455	-5.4332	-15.444
3	-1	-9.0448	-21.602	-6.5742	-8.0922	-5.7850	-10.826
4	-0.5	-7.9953	-11.700	-3.2646	-2.0099	-4.2144	-0.0540
5	0	-7.2010	-7.2309	-2.5794	-3.3320	-4.4168	-1.671
6	0.5	-8.9550	-18.707	-5.3317	-5.3456	-5.9516	-12.587
7	1	-8.0374	-22.157	-5.8305	-11.59	-5.1307	-15.04
8	1.5	-5.4672	-17.602	-4.0195	-11.29	-3.3719	-11.739
9	2	-3.3808	-12.248	-2.3846	-8.664	-2.0619	-8.0732
S.No	Bq	NICS (Hydroxy ring)					
		Neutral isotropic	Neutral anisotrpic (zz)	Cation isotropic	Cation anisotropic (zz)	Anion isotropic	Anion aniotropic (zz)
10	-2	-3.7273	-12.6847	-2.4620	-8.7313	- 2.1368	-8.2104
11	-1.5	-5.7703	-17.1619	-3.7480	-10.672	-3.3663	-10.416
12	-1	-7.7952	-18.8506	-4.7311	-9.1567	-4.4827	-9.4909
13	-0.5	-7.6743	-11.3889	-3.4846	- 0.4975	-3.8366	-0.1390
14	0	-6.3241	-2.8893	- 1.3277	-7.6665	-2.4008	-9.2700
15	0.5	-7.5814	-10.3784	-2.7814	-2.7657	-3.5985	-1.5627
16	1	-7.8909	-18.4326	-4.9384	-7.2498	-4.3909	-8.4815
17	1.5	-5.8887	-17.2223	-4.2797	-10.689	-3.3720	-10.199
18	2	-3.7694	-12.8453	-2.7617	-9.3276	-2.1177	-8.2816
S.No	Bq	NICS (Pyridine ring)					
		Neutral isotropic	Neutral anisotrpic (zz)	Cation isotropic	Cation anisotropic (zz)	Anion isotropic	Anion aniotropic (zz)
19	-2	-3.3690	-11.6986	-4.6594	-15.387	-3.4464	-11.933
20	-1.5	-5.4236	-17.2070	-7.3522	-21.717	-5.3588	-16.369
21	-1	-8.1890	-23.1966	-9.8192	-9.819	-6.8501	- 17.510
22	-0.5	-9.6618	-23.2955	-8.9578	-17.787	-5.2101	-8.1444
23	0	-7.3120	-12.2439	-6.8043	-9.3964	-2.7648	-0.9280
24	0.5	-6.7052	-10.2314	-9.1768	-18.953	-5.2366	-8.8201
25	1	-9.3373	-21.9983	-9.7217	-25.423	- 6.7158	-17.578
26	1.5	-8.6166	-24.2173	-7.1448	-21.28	-5.2172	-16.198
27	2	-5.9355	-18.6672	-4.5372	-14.9578	- 3.3459	-11.828

Table No.S6: Harmonic oscillator model of aromaticity DFT-B3LYP/6-311+G (d, p) calculated HOMA for compounds 1 and 2

S.No	Compound state	Component	HOMA 1	Component	HOMA 2
1	Neutral	Aniline ring	0.9572	Anilide ring	0.9642
		Hydroxy ring	0.9632	Hydroxy ring	0.8932
		Pyridine ring	0.7510	Pyridine ring	0.6350
2	Anion	Aniline ring	0.9471	Anilide ring	0.9642
		Hydroxy ring	0.8807	Hydroxy ring	0.8932
		Pyridine ring	0.5288	Pyridine ring	0.635
3	Cation	Aniline ring	0.7187	Anilide ring	0.7642
		Hydroxy ring	0.8402	Hydroxy ring	0.6712
		Pyridine ring	0.7434	Pyridine ring	0.6335

Table No.S7: Calculated local reactivity properties of compound 1 using B3LYP/6-311+G (d, p) method for Mulliken derived charges

Atoms	fk+	fk-	Δfk(r)	sk+	sk-	sk+/sk-	Δsk (r)	ωk+	ωk-	Δωk(r)
C1	-0.0236	-0.0039	-0.0197	-0.0035	-0.0006	6.0038	-0.0029	-0.0535	-0.0089	-0.0446
C2	1.8895	-0.4468	2.3363	0.2766	-0.0654	-4.2294	0.3420	-0.0535	-1.0139	0.9604
C3	-0.1848	-0.1002	-0.0846	-0.0271	-0.0147	1.8443	-0.0124	-0.4194	-0.2274	-0.1920
C4	0.0543	-0.1603	0.2146	0.0079	-0.0235	-0.3384	0.0314	0.1231	-0.3638	0.4870
C5	-0.0334	0.0283	-0.0618	-0.0049	0.0041	-1.1802	-0.0090	-0.0759	0.0643	-0.1402
C6	0.0816	0.1563	-0.0748	0.0119	0.0229	0.5217	-0.0109	0.1851	0.3548	-0.1697
N11	0.0447	0.1649	-0.1202	0.0065	0.0241	0.2709	-0.0176	0.1014	0.3743	-0.2729
N12	0.7519	-0.6322	1.3841	0.1101	-0.0926	-1.1894	0.2026	1.7065	-1.4347	3.1413
C13	0.0244	-0.0514	0.0758	0.0036	-0.0075	-0.4748	0.0111	0.0554	-0.1166	0.1720
C14	0.1259	0.4232	-0.2973	0.0184	0.0620	0.2975	-0.0435	0.2857	0.9604	-0.6747
C15	-0.0023	-0.0425	0.0402	-0.0003	-0.0062	0.0546	0.0059	-0.0053	-0.0964	0.0912
C16	-0.2186	-0.5338	0.3152	-0.0320	-0.0781	0.4095	0.0461	-0.4961	-1.2114	0.7154
C18	0.1255	0.0835	0.0419	0.0184	0.0122	1.5017	0.0061	0.2847	0.1896	0.0951
C20	-0.0157	0.1793	-0.1950	-0.0023	0.0263	-0.0874	-0.0285	-0.0356	0.4069	-0.4425
O22	0.0203	0.0787	-0.0583	0.0030	0.0115	0.2587	-0.0085	0.0462	0.1785	-0.1323
N24	0.0226	0.0106	0.0120	0.0033	0.0015	2.1366	0.0018	0.0512	0.0240	0.0272
C27	0.1449	-0.0256	0.1705	0.0212	-0.0037	-5.6579	0.0250	0.3288	-0.0581	0.3869
N29	0.1202	-0.0225	0.1427	0.0176	-0.0033	-5.3521	0.0209	0.2729	-0.0510	0.3238
C30	0.0786	0.0537	0.0249	0.0115	0.0079	1.4629	0.0036	0.1783	0.1219	0.0564
C31	-1.0000	1.0541	-2.0541	-0.1464	0.1543	-0.9487	-0.3007	-2.2695	2.3923	-4.6618
C32	0.0030	0.0108	-0.0078	0.0004	0.0016	0.2745	-0.0011	0.0067	0.0245	-0.0178
C33	0.0019	-0.0694	0.0713	0.0003	-0.0102	-0.0274	0.0104	0.0043	-0.1575	0.1618
C35	0.3785	-0.3102	0.6886	0.0554	-0.0454	-1.2201	0.1008	0.8589	-0.7039	1.5629
N39	-0.0054	0.0039	-0.0093	-0.0008	0.0006	-1.3901	-0.0014	-0.0122	0.0088	-0.0210

Table No.S8: Calculated local reactivity properties of compound 2 using B3LYP/6-311+G (d, p) method for Mulliken derived charges

Atoms	fk+	fk-	Δfk(r)	sk+	sk-	sk+/sk-	Δsk (r)	ωk+	ωk-	Δωk(r)
C1	-0.3351	-0.0164	-0.3187	-0.0970	-0.0048	20.389	-0.0922	-1.8721	-0.0918	-1.7803
C2	0.0125	-0.0678	0.0803	0.0036	-0.0196	-0.1848	0.0232	0.0700	-0.3787	0.4487
C3	-0.0600	0.1401	-0.2001	-0.0174	0.0405	-0.4285	-0.0579	-0.3353	0.7825	-1.1179
C4	-0.1235	0.2344	-0.3579	-0.0357	0.0678	-0.5268	-0.1036	-0.6898	1.3093	-1.9990
C5	0.3415	-0.0705	0.4121	0.0988	-0.0204	-4.8440	0.1192	1.9079	-0.3939	2.3018
C6	0.3019	-0.1323	0.4341	0.0874	-0.0383	-2.2817	0.1256	1.6862	-0.7390	2.4252
C21	0.0660	-0.1367	0.2027	0.0191	-0.0396	-0.4832	0.0587	0.3689	-0.7636	1.1325
C22	-0.0931	0.1592	-0.2523	-0.0269	0.0461	-0.5849	-0.0730	-0.5201	0.8893	-1.4094
C23	0.0951	0.0415	0.0536	0.0275	0.0120	2.2892	0.0155	0.5313	0.2321	0.2992
C24	-0.2138	-0.0630	-0.1508	-0.0619	-0.0182	3.3927	-0.0436	-1.1942	-0.3520	-0.8422
C26	-0.1355	0.0001	-0.1355	-0.0392	0.0000	0.0000	-0.0392	-0.7567	0.0004	-0.7571
C28	0.2741	-0.0321	0.3062	0.0793	-0.0093	-8.5403	0.0886	1.5312	-0.1793	1.7105
C35	0.0163	0.1456	-0.1292	0.0047	0.0421	0.1122	-0.0374	0.0912	0.8132	-0.7220
C36	-0.0140	0.0741	-0.0881	-0.0040	0.0215	-0.1886	-0.0255	-0.0781	0.4142	-0.4923
C37	0.0004	-0.0062	0.0066	0.0001	-0.0018	-0.0597	0.0019	0.0021	-0.0347	0.0368
C38	0.0379	-0.0803	0.1181	0.0110	-0.0232	-0.4717	0.0342	0.2115	-0.4484	0.6600
C40	0.0258	0.0400	-0.0142	0.0075	0.0116	0.6455	-0.0041	0.1443	0.2235	-0.0792
N44	0.9980	-0.0112	1.0092	0.2888	-0.0032	-89.107	0.2921	5.5749	-0.0626	5.6375

Table No.S9: Calculated maximum absorption wavelength of compound 1 in various solvents

S.No	Solvent	ΔE (eV)	f (a.u)	λ_{max} (nm)	Types and % of transition
1	Gas	3.03	0.30	492	H→L (89) H→L+1(7)
2		3.22	0.74	373.2	H→L(7) H→L+1(90)
3	Benzene	2.94	0.63	422.1	H→L(90) H→L+1(7)
4		3.20	0.57	387.8	H→L (7) H→L+1(91)
5	DCM	2.90	0.67	426.5	H→L(89) H→L+1(7)
6		3.19	0.50	388.7	H→L(7) H→L+1(90)
7	Chloroform	2.92	0.65	424.8	H→L(89) H→L+1(7)
8		3.19	0.53	388.4	H→L(7) H→L+1(90)
9	Acetone	2.91	0.66	426.7	H→L (89) H→L+1(7)
10		3.19	0.49	388.1	H→L(8) H→L+1(89)
11	Ethanol	2.9	0.67	427.0	H→L(89)

					H→L+1(7)
12		3.2	0.49	388.2	H→L(8) H→L+1(90)
13	Methanol	2.90	0.65	426.6	H→L(89) H→L+1(7)
14		3.20	0.50	387.7	H→L(8) H→L+1(90)
15	Acetonitrile	2.9	0.66	427.0	H→L(89) H→L+1(7)
16		3.16	0.49	388.0	H→L(36) H→L+1(90)
17	DMSO	2.89	0.69	428.7	H→L(89) H→L+1(7)
18		3.19	0.47	389.3	H→L(8) H→L+1(90)
19	Water	2.90	0.66	427.2	H→L(89) H→L+1(7)
20		3.2	0.48	387.9	H→L(8) H→L+1(90)

Table No.S10: Calculated and experimental maximum absorption wavelength of compound 2 in various solvents

S.No	Solvent	ΔE (eV)	f (a.u)	λ_{max} (nm)	Types and % of transition	Experimental λ_{max} (nm)
1	Gas	3.21	0.89	386.4	H→L (97)	
2		3.31	0.48	374.7	H→L+1(23)	
3	Benzene	3.08	1.24	402.5	H→L (97)	
4		3.31	0.33	374.4	H→L+1(98)	360.7
5	DCM	3.08	1.21	402.1	H→L(97)	
6		3.35	0.32	370.5	H→L+1(93)	355
7	Chloroform	3.08	1.22	402.1	H→L(97)	
8		3.33	0.32	371.8	H→L+1(93)	358.8
9	Acetone	3.09	1.19	400.9	H→L(97)	
10		3.36	0.31	369.4	H→L+1(93)	359
11	Ethanol	3.09	1.195	401.1	H→L(97)	
12		3.36	0.31	369.3	H→L+1(93)	359,247
13	Methanol	3.1	1.18	400.3	H→L(97)	359,239
14		3.36	0.31	369.0	H→L+1(98)	
15	Acetonitrile	3.09	1.189	400.7	H→L(97)	357,241.3
16		3.36	0.308	369.1	H→L+1(93)	
17	DMSO	3.08	1.21	402.6	H→L(97)	475sh
18		3.36	0.31	369.4	H→L+1(98)	386
19	Water	3.096	1.185	400.5	H→L(97)	
20		3.362	0.307	368.8	H→L+1(93)	362.6

Table No.S11: Solvent effect of 1 on dielectric constant, dipole moment, energy, hyperpolarisablity and polarisablity

S.No	Solvent	Dielectric constants	Dipole moment (Debye)	Energy (Hartree)	Hyperpolarisability β x10^{30}	Polarisability Δα x 10^{24}	ΔG (kcal/mol)
1	Gas phase	0	2.7054	-1044.154291	2.30291	10.0000	0
2	Benzene	2.28	3.0656	-1044.163148	2.56177	11.4730	-5.55821
3	Chloroform	4.81	3.3081	-1044.168978	2.71108	12.5000	-9.21649
4	Dichloromethane	9.08	3.4562	-1044.172299	2.78914	13.1060	-11.3001
5	Acetone	21.01	3.5727	-1044.174732	2.84320	13.5610	-12.8270
6	Ethanol	24.6	3.5904	-1044.175086	2.85084	13.6280	-13.0492
7	Methanol	32.6	3.6108	-1044.17549	2.85949	13.7040	-13.3024
8	Acetonitrile	36.64	3.6166	-1044.175603	2.86190	13.7260	-13.3732
9	DMSO	47	3.6313	-1044.17589	2.86800	13.7800	-13.5535
10	Water	78	3.6509	-1044.176267	2.87594	13.8520	-13.7899

Table No.S12: Solvent effect of 2 on dielectric constant, dipole moment, energy, hyperpolarisablity and polarisablity

S.No	Solvent	Dielectric constants	Dipole moment (Debye)	Energy (Hartree)	Hyperpolarisability β x10^{30}	Polarisability Δα x 10^{24}	ΔG(kcal/mol)
1	Gas phase	0	4.2684	-1196.871432	5.81505	10.8819	0
2	Benzene	2.28	4.7507	-1196.880264	6.38826	12.2422	-5.5425
3	Chloroform	4.81	5.0564	-1196.885697	6.68840	13.1134	-8.95173
4	Dichloromethane	9.08	5.2347	-1196.888663	6.83513	13.6025	-10.8126
5	Acetone	21.01	5.3696	-1196.890778	6.93234	13.9579	-12.1398
6	Ethanol	24.6	5.3896	-1196.891081	6.94578	14.0094	-12.3302
7	Methanol	32.6	5.4125	-1196.891426	6.96090	14.0680	-12.5465
8	Acetonitrile	36.64	5.4189	-1196.891522	6.96508	14.0844	-12.607
9	DMSO	47	5.4354	-1196.891767	6.97566	14.1261	-12.7604
10	Water	78	5.457	-1196.892086	6.98936	14.1807	-12.9608

Table No.S13: Theoretical ^{1}H and ^{13}C chemical shifts of compounds 1 and 2

S.No	Atoms	Theoritical chemical shifts(ppm)	Atoms	Theoritical chemical shifts(ppm)	Atoms	Theoritical chemical shifts (ppm)	Atoms	Theoritical chemical shifts (ppm)
	1				2			
1	H17	9.19	C27	155.03	H31	13.65	C35	169.91
2	H36	8.80	C13	153.31	H41	8.81	C32	168.40
3	H28	8.49	C3	151.50	H33	8.66	C37	155.93
4	H19	8.21	C15	143.89	H27	8.37	C3	155.14
5	H8	8.14	C4	142.31	H9	8.24	C21	151.42
6	H9	8.04	C33	141.94	H25	8.07	C6	147.17
7	H37	7.66	C16	124.96	H8	8.06	C22	144.08
8	H21	7.25	C35	122.71	H42	7.80	C38	142.30
9	H38	7.06	C18	120.00	H43	7.20	C2	140.04
10	H10	6.78	C2	119.80	H29	7.18	C5	125.80

11	H7	6.65	C14	118.42	H10	7.18	C23	125.73
12	H34	6.60	C1	117.37	H39	7.06	C1	124.78
13	H23	5.30	C5	115.42	H7	7.00	C40	124.45
14	H26	3.48	C31	114.61	H12	6.68	C24	123.30
15	H25	3.46			H17	2.15	C26	122.77
16	C30	173.77			H16	2.15	C4	118.50
17	C20	165.96			H18	1.90	C36	115.48
18	C6	155.59			C28	173.91	C15	21.24
19	C32	155.44			C13	172.39		

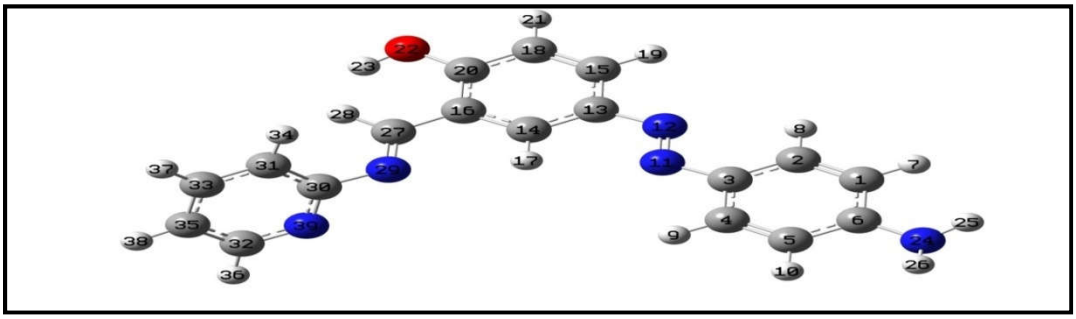

Compounds 1

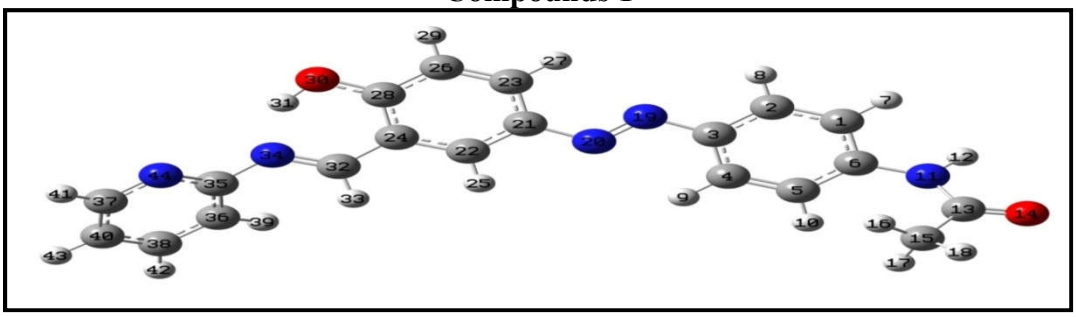

Compounds 2

Figure No.1: Optimized structure of compounds 1 and 2

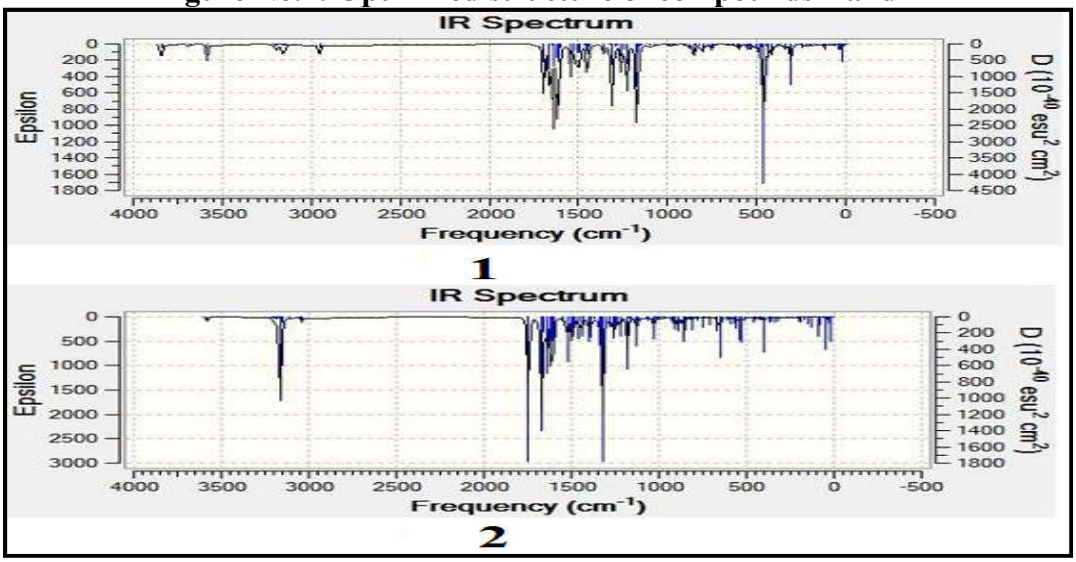

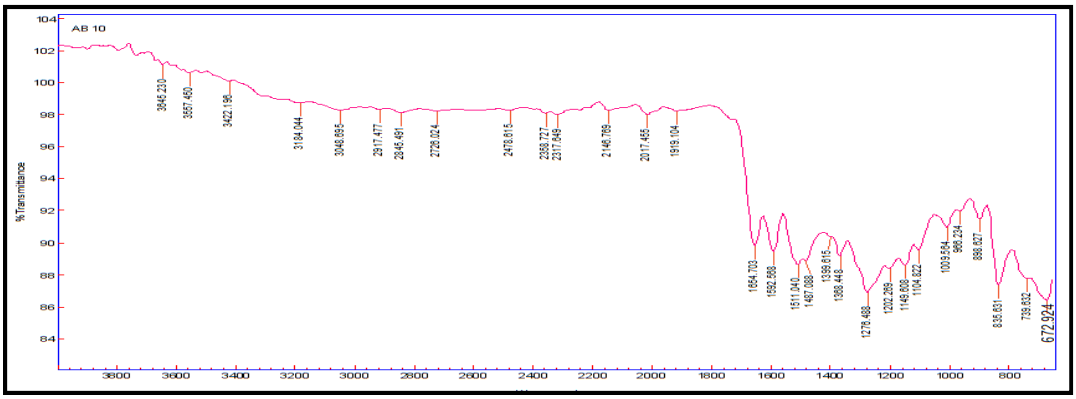

Figure No.2: Theoretical IR spectra of compounds 1 and 2 and experimental spectrum of compound 2 in KBr disc (cm^{-1})

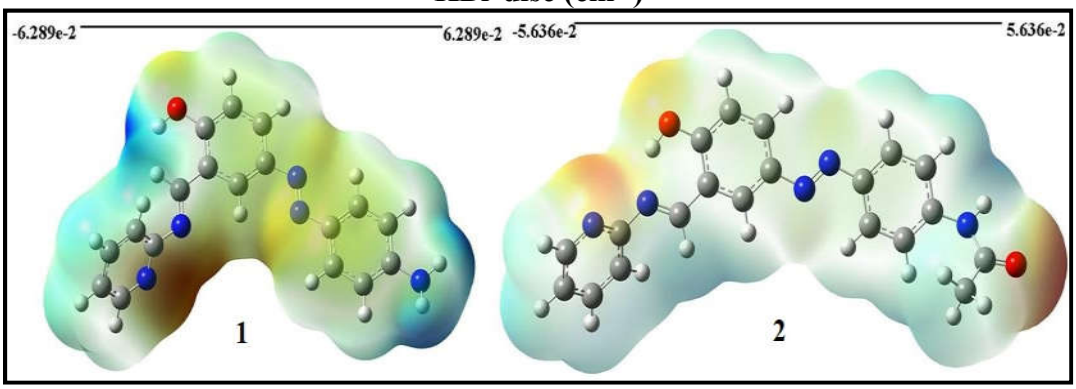

Figure No.3: MEP of compounds 1 and 2

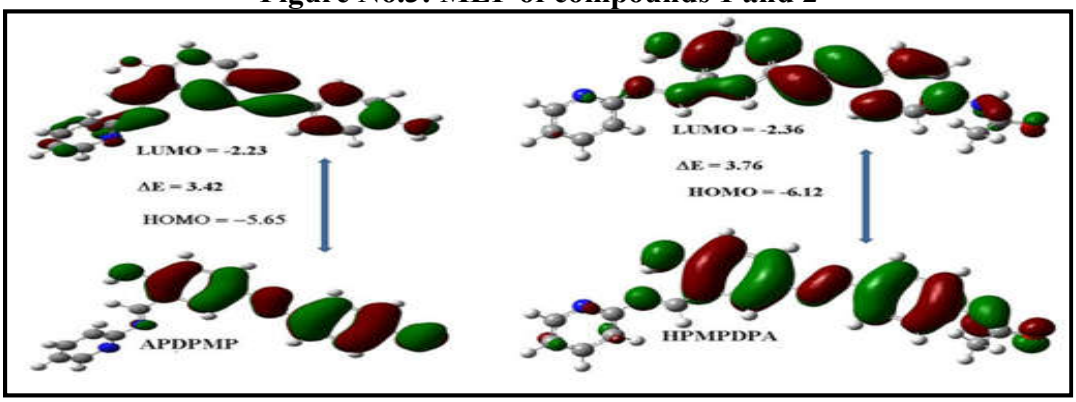

Figure No.4: HOMO-LUMO plots of compounds 1 and 2

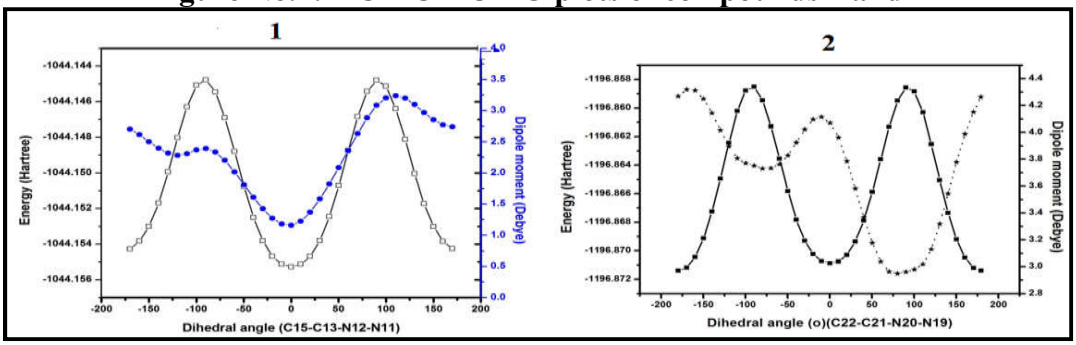

Figure No.5: Plot of dihedral angle Vs energy and dipole moment for 1 and 2

CONCLUSION

In this work, we explored the structure of molecule, their aromatic indices NICS, HOMA and they are accounted using HOMO-LUMO lobe concentration. The compounds also studied for Mulliken charges and Fukui function. Change in properties like dipole moment, polarisability and hyperpolarisability were discussed vastly with change in solvent and change in dihedral angle. It is found that the dipole, polarisability and hyperpolarisability value increases with incerease in dielectric constants, and also with increase in planarity of the molecule. The NLO properties are much higher for the compound 2 under study. Compared with literature they are found to be competitive candiadates for the NLO study. Planarity of 2 is also found to be greater than 1 and it is portrayed in its properties. Solvation energy data is found to be more negative for 1 and it can act as a good drug.

ACKNOWLEDGEMENT

We are thankful to the Department of Chemistry, Annamalai University, Chidambaram for providing lab and instrumental facilities.

CONFLICT OF INTEREST

We declare that we have no conflict of interest.

BIBLIOGRAPHY

1. Kumar J, Rai A. A comprehensive review on the pharmacological activity of schiff base containing derivatives, *Org. Med. Chem. Int. J,* 1(3), 2017, 1-15.
2. Da Silva C M, Alves R B. Schiff bases: A short review of their antimicrobial activities, *J. Adv. Res,* 2(1), 2011, 1-8.
3. Kajal A. Schiff bases: A versatile pharmacophore, *J. Ca,* 2013, Article ID: 893512, 2013, 1-14.
4. Ebrahimipour S Y, Rudbari, Bruno G, Janiak C. Mono- and dioxido-vanadium (V) complexes of a tridentate ONO Schiff base ligand: Synthesis, spectral characterization, X-ray crystal structure and anticancer activity, *Poly,* 93, 2015, 99-105.
5. Chacko S, Samanta S. A novel approach towards design, synthesis and evaluation of some Schiff base analogues of 2-aminopyridine and 2-aminobezothiazole against hepatocellular carcinoma, *Biomed. Pharmacother,* 89, 2017, 162-176.
6. Sondhi S M, Singh N, Kumar A, Lozach O, Meijer L. Synthesis, anti-inflammatory, analgesic and kinase (CDK-1, CDK-5 and GSK-3) inhibition activity evaluation of benzimidazole/benzoxazole derivatives and some Schiff's bases, *Bioorg. Med. Chem,* 14(11), 2006, 3758-3765.
7. Chandramouli C, Shivanand M R, Nayanbhai T B, Bheemachari, Udupi R H. Synthesis and biological screening of certain new triazole schiff bases and their derivatives bearing substituted benzothiazole moiety, *J. Chem. Pharm. Res,* 4(2), 2012, 1151-1159.
8. Chinnasamy R P, Sundararajan R and Govindaraj S. Synthesis, characterization, and analgesic activity of novel Schiff base of isatin derivatives, *J. Adv. Pharm. Tech. Res,* 1(3), 2010, 342-347.
9. Mermer A, Demirbas N, Uslu H, Demisbas A, Ceylan S, Sirin Y. Synthesis of novel Schiff bases using green chemistry techniques; Antimicrobial, antioxidant, antiurease activity screening and molecular docking studies, *J. Mol. Struct,* 1181, 2019, 412-422.
10. Wang P H, Keck J G, Lien E J and Lai M M C. Design, synthesis, testing, and quantitative structure-activity relationship analysis of substituted salicylaldehyde Schiff bases of 1-amino-3-hydroxyguanidine tosylate as new antiviral agents against coronavirus, *J. Med. Chem,* 33(2), 1990, 608-614.
11. Chaubey A K. Synthesis and anticonvulsant activity (chemo shock) of Schiff and mannich bases of isatin derivatives with 2-amino pyridine (Mechanism of Action), *Int. J. Pharm. Tech. Res,* 4(2), 2012, 590-598.
12. Al Zoubi W, Al-Hamdani A A S, Ahmed S D, Ko Y G. Synthesis, characterization, and biological activity of Schiff bases metal

complexes, *J. Phys. Org. Chem,* 31(2), 2018, 1-13.

13. Garg G, Acharya A, Patel K. Synthesis and biological evaluation of some Schiff base ligand as antimalarial agents, *Int. J. Biomed. Res,* 4(3), 2013, 137-144.
14. Aboul-Fadl T, Mohammed F A, Hassan E A. Synthesis, antitubercular activity and pharmacokinetic studies of some Schiff bases derived from 1-alkylisatin and isonicotinic acid hydrazide (INH), *Arch. Pharmacol. Res,* 26(10), 2003, 778-784.
15. Wang X, Yin J, Shi L, Zhang G, Song B. Design, synthesis, and antibacterial activity of novel Schiff base derivatives of quinazolin-4(3H)-one, *Eur. J. Med. Chem,* 77(C), 2014, 65-74.
16. Wei D, Li N, Lu G, Yao K. Synthesis, catalytic and biological activity of novel dinuclear copper complex with Schiff base, *Sci. Chin. Series B: Chem,* 49(3), 2006, 225-229.
17. Avaji P G, Kumar C H V, Patil S A, Shivananda K N, Nagaraju C. Synthesis, spectral characterization, *in-vitro* microbiological evaluation and cytotoxic activities of novel macrocyclic bishydrazone, *Eur. J. Med Chem,* 44(9), 2009, 3552-3559.
18. Katritzky A R, Dennis N. Cycloaddition reactions of heteroaromatic six-membered rings, *Chem. Rev,* 89(4), 1989, 827-867.
19. Schantl J G. Cyclic azomethine imines from diazenes (AZO Compounds), *Adv. Heterocyclic Chem,* 99, 1st Edition, 2010, 185207.
20. Tabarrini O, Manfroni G, Fravolini A, Cecchetti V, Sabatini S, De Clercq E, Rozenski J, Canard B, Dutartre H, Paeshuyse J, Neyts J. Synthesis and anti-BVDV activity of acridones as new potential antiviral agents, *J. Med. Chem,* 49(8), 2006, 2621-2627.
21. Balzarini J, Stevens M, Clercq E D, Schols D, Pannecouque C. Pyridine N-oxide derivatives: Unusual anti-HIV compounds with multiple mechanisms of antiviral action, *J. Antimicrob. Chemother,* 55(2), 2005, 135-138.
22. Cocco M T, Congiu C, Lilliu V, Onnis V. Synthesis and antiproliferative activity of 2, 6-dibenzylamino-3, 5-dicyanopyridines on human cancer cell lines, *Eur. J. Med. Chem,* 40(12), 2005, 1365-1372.
23. Mauro V D A, Marcus V N S, Nadia R B, Frederico P S, Giovanni W A, Sílvia H C. Synthesis and antimicrobial activity of pyridine derivatives substituted at C-2 and C-6 positions, *Lett. Drug Des. Discov,* 4(2), 2007, 149-153.
24. Mauricio Alcolea Palafox. Scaling factors for the prediction of vibrational spectra. I. Benzene molecule, *Int. J. Quantum Chem,* 77(3), 2000, 661-684.
25. Michal H. Jamroz. Vibrational energy distribution analysis VEDA4, *Warsaw,* 2004-2010, https://smmg.pl/software/veda.
26. Snehalatha M, Sekar N, Hubert Joe I, Jayakumar V S. Quantum chemical computations and Fourier transform infrared spectral studies of a nonlinear food dye E110, *Spectrochim. Acta A,* 69(1), 2008, 82-90.
27. Mohammed Bakir, Gabriel R. Harewood, Alvin Holder, Ishmael Hassan, Tara P Dasgupta, Paul Maragh, Marvadeen Singh-Wilmot. 5-[(4-methylphenyl)diazenyl]salicylaldehyde, *Acta Crystallogr, E*61(6), 2005, o1611-o1613.
28. Biswas N, Umapathy S. Density functional calculations of structures, vibrational frequencies, and normal modes of *trans*- and *cis*-Azobenzene, *J. Phys. Chem. A,* 101(30), 1997, 5555-5566.
29. Dos Santos H F, De Oliveira L F C, Dantas S O, Santos P S, De Almeida W B. Quantum mechanical investigation of the tautomerism in the AZO dye Sudan III, *Int. J. Quantum Chem,* 80(4-5), 2000, 1076-1086.
30. Nevzat Karaday, Cigdem Albayrak, Mustafa Odabasoglu, Orhan Buyukgungor. (*E*)-5-[(3-Chlorophenyl) diazenyl]-2-hydroxy-3-methoxybenzaldehyde, *Acta Crystallogr,* E62(9), 2006, o1699-o1701.
31. Sudha N, Anbuselvi S, Sudhakar Jyothula, Thiruppathi A, Vijayakumar B, Kartikeya

Parmar, Puthilibai G, Leevesh Kumar. Synthesis, structural, spectroscopic, Hirshfeld surface analysis and DFT investigation of benzaldehydesemicarbazone, *Adv. Mater. Sci. Eng,* 2022, Article ID: 4091119, 2022, 1-14.

32. Smith B. Infrared spectral interpretation, a systematic approach, *CRC Press, Washington, DC,* 1st Edition, 1999, 304.
33. Silverstein R M, Webster F X. Spectroscopic identification of organic compounds, *John Wiley and Sons Inc, New York,* 6th Edition, 2003, 1-495.
34. Bellamy L J. The infra-red spectra of complex molecules, *Chapman and Hall, London,* 1980, 299.
35. Vandenabeele P, Moens L, Edwards H G M, Dams R. Raman spectroscopic database of azo pigments and application to modern art studies, *J. Raman Spectrosc,* 31(6), 2000, 509-517.
36. Trotter P J. Azo dye tautomeric structures determined by Laser-Raman Spectroscopy, *Appl. Spectrosc,* 31(1), 1977, 30-35.
37. Snehalathaa M, Ravikumar C, Hubert Joea I, Sekar N and Jayakumar V S. Spectroscopic analysis and DFT calculations of a food additive carmoisine, *Spectrochim. Acta A,* 72(3), 2009, 654-662.
38. Lana O. Ahmed, Rebaz A, Omer. Population analysis and UV-Vis spectra of dopamine molecule using Gaussian 09, *JPCFM,* 3(2), 2020, 48-58.
39. Obi-Egbedi N O, Obot I B and El-khaiary M I. Quantum chemical investigation and statistical analysis of the relationship between corrosion inhibition efficiency and molecular structure of xanthene and its derivatives on mild steel in sulphuric acid, *J. Mol. Struct,* 1002(1-3), 2011, 86-96.
40. Obot I B, Johnson A S. *Ab initio*, DFT and TD-DFT electronic absorption spectra investigations on 3, 5-diamino-1, 2, 4-triazole, *Comp. Chem,* 43, 2012, 6658-6661.
41. Ravikumar C, Hubert Joe I, Sajan D. Vibrational contributions to the second-order nonlinear optical properties of π-conjugated structure acetoacetanilide, *Chem. Phys,* 369(1), 2010, 1-7.
42. Ravikumar C, Hubert Joe I and Jayakumar V S. Charge transfer interactions and nonlinear optical properties of push-pull chromophorebenzaldehyde-phenylhydrazone: A vibrational approach, *Chem. Phys. Lett,* 460(4-6), 2008, 552-558.
43. Zeynep Demircioglu, Cigdem Albayrak Kastas, Orhan Buyukgungor. Theoretical analysis (NBO, NPA, Mulliken population method) and molecular orbital studies (hardness, chemical potential, electrophilicity and Fukui function analysis) of (E)-2-((4-hydroxy-2-methylphenylimino) methyl)-3-methoxyphenol, *J. Mol. Struct,* 1091(5), 2015, 183-195.
44. Politzer P, Concha M C and Murray J S. Density functional study of dimers of dimethylnitramine, *Int. J. Quantum Chem,* 80(2), 2000, 184-192.
45. Anitha L, Saritha S R, Layana S R, Nair Lakshmi C S, Hubert Joe I and Sudarsanakumar M R. Structural studies of 3-[(*E*)-[(2(*E*)-2-methyl-3-phenylprop-2-en-1-ylidene] amino]-1-phenylthiourea: Combined experimental and computational studies, *J Mol. Struc,* 1197, 2019, 206-217.
46. Jezierska-Mazzarello A, Panek J J, Szatyłowicz H and Krygowski T M. Hydrogen bonding as a modulator of aromaticity and electronic structure of selected *ortho*-hydroxybenzaldehyde derivatives, *J. Phys. Chem. A,* 116(1), 2012, 460-475.
47. Kruszewski J and Krygowski T M. Definition of aromaticity basing on the harmonic oscillator model, *Tetrahedron Lett,* 13(36), 1972, 3839-3842.
48. Krygowski T M. Crystallographic studies of inter- and intra-molecular interactions reflected in aromatic character of π.-electron systems, *J. Chem. Inf. Model,* 33(1), 1993, 70-78.
49. Eduard Matito, Jordi Poater, Miquel Durana, Miquel Sola. An analysis of the changes in

aromaticity and planarity along the reaction path of the simplest Diels–Alder reaction, Exploring the validity of different indicators of aromaticity, *J. Mol. Struct. Theochem,* 727(1-3), 2005, 165-171.

50. Zhongfang Chen, Chaitanya S. Wannere, Cle´mence Corminboeuf, Ralph Puchta and Paul von Ragueˊ Schleyer. Nucleus-independent chemical shifts (NICS) as an aromaticity criterion, *Chem. Rev,* 105(10), 2005, 3842-3888.
51. Sławomir Ostrowski, Jan Cz. Dobrowolski. What does the HOMA index really measure? *RSC Adv,* 4(83), 2014, 44158-44161.
52. Parr R G, Yang W. Density functional approach to the frontier-electron theory of chemical reactivity, *J. Am. Chem. Soc,* 106(14), 1984, 4049-4050.
53. Yang W, Mortier W J. The use of global and local molecular parameters for the analysis of the gas-phase basicity of amines, *J. Am. Chem. Soc,* 108(19), 1986, 5708-5711.
54. Arzu Ozek Yildirim, Hakki Yildirim M, Cigdem Albayrak Kastas. Studies on the synthesis, spectroscopic analysis and DFT calculations on (*E*)-4, 6-dichloro-2-[(2-chlorophenylimino)methyl]-3-methoxyphenol as a novel Schiff's base, *J. Mol. Struct,* 1113, 2016, 1-8.
55. Thanthiriwatte K S, Nalin De Silva K M. Non-linear optical properties of novel fluorenyl derivatives-*ab initio* quantum chemical calculations, *J. Mol. Struct. Theochem,* 617(1-3), 2002, 169-175.
56. Schwenke D W, Truhlar D G. Systematic study of basis set superposition errors in the calculated interaction energy of two HF molecules, *J. Chem. Phys,* 82(5), 1985, 2418-2426.
57. Arockiadoss M, Savithiri S, Rajarajan G, Thanikachalam V, Saleem H. Synthesis, spectroscopic (FT-IR, FT-Raman, UV and NMR) and computational studies on 3*t*-pentyl-2*r*, 6*c*-diphenylpiperidin-4-one semicarbazone, *Spectrochim. Acta A,* 148, 2015, 189-202.
58. Arockia Doss M, Amala S, Rajarajan G, Thanikachalam V. Synthesis, spectral (Uv-Vis, FT-IR and NMR), molecular structure, NBO, HOMO-LUMO and NLO Analysis of Some *3t*-pentyl-*2r*, *6c*-diarylpiperidin-4-one Semicarbazones, *Can. Chem. Trans,* 4(3), 2016, 398-414.
59. Saritha S R, Anitha L, Layana S R, Sudarsanakumar M R, Hubert Joe I, Manimaran D, Siji V L. Spectral, structural and theoretical studies of α–methyl *trans*-cinnamaldehydesemicarbazone, *J. Mol. Struct,* 1182, 2019, 329-339.
60. Snehalatha M, Ravikumar C, Hubert Joe I, Sekar N, Jayakumar V S. Spectroscopic analysis and DFT calculations of a food additive carmoisine, *Spectrochim. Acta A,* 72(3), 2009, 654-662.
61. Mizuseki H, Igarashi N, Majumder C, Belosludov R, Farajian V, Kawazoe A, Y. Theoretical study of donor-spacer-acceptor structure molecule for use as stable molecular rectifier: Geometric and electronic structures, *Thin Solid Films,* 438, 2003, 235-237.
62. Tian Lu, Feiwu Chen. Multiwfn: A multifunctional wave function analyzer, *J. Comput. Chem,* 33(5), 2012, 580-592.
63. Dutta A, Jana A D, Gagopadhyay S, Das K K, Marek J, Marek R, Brus J, Ali M. Unprecedented π···π interaction between an aromatic ring and a pseudo-aromatic ring formed through intra-molecular H-bonding in a bidentate Schiff base ligand: crystal structure and DFT calculations, *Phys. Chem. Chem. Phys,* 13(35), 2011, 15845-15853.
64. Binil P S, Anoop M R, Jisha K R, Suma S, Sudarsanakumar M R. Growth, spectral and thermal characterization of vanillin semicarbazone (VNSC) single crystals, *J. Therm. Anal. Calorim,* 111(1), 2013, 575-581.
65. Rakesh Maity, Debkumar Mandal, Ajay Misr A. Role of π electron conjugation in determining the electrical responsive properties of polychlorinated biphenyls: A DFT based computational study, *SN Appl. Sci,* 2(3), 2020, 418, 1-11.

66. Mininath S. Deshmukh, Nagaiyan Sekar. A combined experimental and TD-DFT investigation of three disperse AZO dyes having the nitroterephthalate skeleton, *Dyes Pigm,* 103(5), 2014, 25-33.
67. Msugh Targema, Nelson O, Obi-Egbedi, Moriam D. Adeoye. Molecular structure and solvent effects on the dipole moments and polarizabilities of some aniline derivatives, *Comput. Theor. Chem,* 1012, 2013, 47-53.
68. Mazharul M. Islam, Delower M, Bhuiyan H, Thomas Bredow, Andrew C. Try. Theoretical investigation of thenonlinear optical properties of substituted anilines and *N*, *N*-dimethylanilines, *Comput. Theor. Chem,* 967(1), 2011, 165-170.

Please cite this article in press as: Thanikachalam V *et al*. Theoretical and DFT studies of 4-((*E*)-(4-amino-phenyl)diazenyl)-2-((*E*)-(pyridin-2-ylimino)methyl)-phenol and N-(4-((*E*)-(4-hydroxy-3-((*E*)-(pyridin-2-yl-imino)methyl)phenyl)diazenyl)phenyl)acetamide, *Asian Journal of Research in Chemistry and Pharmaceutical Sciences,* 10(2), 2022, 114-150.